Concentrations of tire wear microplastics and other traffic-derived non-exhaust particles in the road environment

Environment International 170 (2022) 107618

Contents lists available at ScienceDirect

Environment International

journal homepage: www.elsevier.com/locate/envint

Full length article

Concentrations of tire wear microplastics and other traffic-derived non-exhaust particles in the road environment

Ida Järlskog [a,b,*], David Jaramillo-Vogel [c], Juanita Rausch [c], Mats Gustafsson [a], Ann-Margret Strömvall [d], Yvonne Andersson-Sköld [a,b]

[a] Swedish National Road and Transport Research Institute (VTI), SE-581 95 Linköping, Sweden
[b] Geology and Geotechnics, Department of Architecture and Civil Engineering, Chalmers University of Technology, SE-412 96 Gothenburg, Sweden
[c] Particle Vision GmbH, Passage du Cardinal 13b, 1700 Fribourg, Switzerland
[d] Water Environment Technology, Department of Architecture and Civil Engineering, Chalmers University of Technology, SE-412 96 Gothenburg, Sweden

ARTICLE INFO

Handling editor: Xavier Querol

Keywords:
Microplastics
TRWP
SEM/EDX
Machine learning
Metal particles
Bitumen particles
Road markings

ABSTRACT

Tire wear particles (TWP) are assumed to be one of the major sources of microplastic pollution to the environment. However, many of the previously published studies are based on theoretical estimations rather than field measurements. To increase the knowledge regarding actual environmental concentrations, samples were collected and analyzed from different matrices in a rural highway environment to characterize and quantify TWP and other traffic-derived non-exhaust particles. The sampled matrices included road dust (from kerb and in-between wheeltracks), runoff (water and sediment), and air. In addition, airborne deposition was determined in a transect with increasing distance from the road. Two sieved size fractions (2–20 μm and 20–125 μm) were analyzed by automated Scanning Electron Microscopy/Energy Dispersive X-ray spectroscopy (SEM/EDX) single particle analysis and classified with a machine learning algorithm into the following subclasses: TWP, bitumen wear particles (BiWP), road markings, reflecting glass beads, metals, minerals, and biogenic/organic particles. The relative particle number concentrations (%) showed that the runoff contained the highest proportion of TWP (up to 38 %). The share of TWP in kerb samples tended to be higher than BiWP. However, a seasonal increase of BiWP was observed in coarse (20–125 μm) kerb samples during winter, most likely reflecting studded tire use. The concentration of the particle subclasses within airborne $PM_{80\text{-}1}$ decreases with increasing distance from the road, evidencing road traffic as the main emission source. The results confirm that road dust and the surrounding environment contain traffic-derived microplastics in both size fractions. The finer fraction (2–20 μm) dominated (by mass, volume, and number) in all sample matrices. These particles have a high potential to be transported in water and air far away from the source and can contribute to the inhalable particle fraction (PM_{10}) in air. This highlights the importance of including also finer particle fractions in future investigations.

1. Introduction

Non-exhaust emissions (NEE) of particles stemming from tires, brakes, road surfaces, and road markings are an important source of environmental pollution (Baensch-Baltruschat et al., 2020). NEE can be divided into several compositional sub-categories: traffic-related organic pollutants such as polyaromatic hydrocarbons (PAH), microplastics (MP) (i.e., rubber from tire wear, plastics from road markings, and polymer-modified bitumen), metal particles (e.g., iron (Fe), copper (Cu), zinc (Zn) and lead (Pb) bearing particles related to many sources, but brake wear being especially dominant), mineral particles derived from road wear, and glass bead fragments from road markings (Amato et al., 2016; Järlskog et al., 2021; Thorpe and Harrison, 2008). In the road environment, particles deposited on the road surface tend to mix and form heterogeneous road dust, which can be resuspended by traffic (Fussell et al., 2022; Padoan and Amato, 2018). Furthermore, particles related to other sources than traffic, such as mineral dust from nearby soils, construction works, quarrying, pollen, spores, and organic matter emitted during biogenic activity are often sedimented on the road surface and can interact with traffic-derived NEE (Fuzzi et al., 2015; Piscitello et al., 2021).

Microplastics are defined as solid, water-insoluble, polymer-based

* Corresponding author at: Swedish National Road and Transport Research Institute (VTI), SE-581 95 Linköping, Sweden.
E-mail address: ida.jarlskog@vti.se (I. Järlskog).

https://doi.org/10.1016/j.envint.2022.107618
Received 28 June 2022; Received in revised form 2 November 2022; Accepted 2 November 2022
Available online 3 November 2022

particles smaller than 5 mm with a low degradation rate (Boucher and Friot, 2017; Verschoor et al., 2016). Tire wear particles, TWP, are often considered microplastic, and recent theoretical estimates suggest that TWP is one of the dominating sources of MP pollution globally (Hann et al., 2018; Hartmann et al., 2019; Kole et al., 2017). In the past, the release of non-exhaust particles into the environment has been mainly estimated by theoretical emission factors (Beddows and Harrison, 2021). The emissions of tire wear particles have been estimated for example based on driving distance, the weight of vehicles (i.e., personal cars or heavy vehicles), speed, tire type, and pavement rather than based on field sampling or monitoring studies (Baensch-Baltruschat et al., 2020). The theoretical emissions of TWP on a global scale were estimated to be 6.000.000 tons per year (Kole et al., 2017).

When the particles have been generated at the road surface through interaction between tire and pavement, the TWP can either sediment at the road edge or enter the environment through road runoff or via air (Baensch-Baltruschat et al., 2020; Sieber et al., 2020; Wagner et al., 2018). Studies have shown that the majority of the coarser particles are deposited on the road edge or in the ditch nearby the road (e.g., Sieber et al., 2020; Wagner et al., 2018). The finer particle fractions can be further transported with road runoff into stormwater systems or through atmospheric transport. However, there is still a knowledge gap, and empirical data is lacking regarding the occurrence and transport of TWP from the road surface into the environment (Knight et al., 2020). Moreover, when MP and TWP have been investigated, other components like in broad sense particulate matter (PM), or specifically minerals, or metals have rarely been included in the same analyses. Yet, since the traffic-derived PM in environmental samples from road environments are intermixed with each other and with particles from other more distal sources, it is important to analyze the wide spectrum of traffic-derived particle types (e.g., MP, metals, and organic pollutants) to achieve a comprehensive understanding of the contribution and transport of traffic-derived pollutants.

Further, tire wear particles (and tire and road wear particles (TRWP) are difficult to analyze, mainly because the particles are black, have a large size range, and have complex chemical composition. Pristine tire treads are rarely found in the environment but are rather encrusted with minerals, bitumen, or other particles, which further complicates the analysis (Halle et al., 2021; Kreider et al., 2010; Unice et al., 2013). During the last years, several methods have been developed for the analysis of TWP and TRWP in environmental samples (e.g., Goβmann et al., 2021; Järlskog et al., 2022; Mengistu et al., 2021; Müller et al., 2022; Rausch et al., 2022; Rødland et al., 2022a), and thermal methods such as pyr-GC/MS and TED-GC/MS are two of the most common methods (Löder and Gerdts, 2015). Still, the existing methods often provide different information, which complicates the comparison between studies (Thomas et al., 2020; Rauert et al., 2021). As an example, some of the recently published studies present a large variation in TWP concentrations in road dust, but the studies have not analyzed the same size ranges and used different analytical methods with different settings and chemical markers (Chae et al., 2021; Knight et al., 2020; Kumata et al., 2002; Rødland et al., 2022a; Youn et al., 2021). It is therefore complicated to apply the results from previous studies to understand the occurrence of TWP in various matrices, and thereby also be able to investigate and understand associated environmental risks.

Thermal methods also destruct the samples, resulting in a loss of information regarding the number of particles, particle size distribution, and physical properties of the particles, which is of importance to increase the understanding of transport routes and environmental effects. There is also a lack of empirical studies about the occurrence of traffic-derived microplastics in different matrices in the road environment related to the properties of the particles. Such information is further essential to be able to model the potential transport in the environment, and as pointed out by Mennekes and Nowack (2022), an improved understanding of TWP quantities would also result in a better management of the risk of environmental pollution.

This study aims to investigate the abundance and examine the occurrence and composition of traffic-derived microplastics and other road-related particles in multiple sample matrices (road dust, runoff, sediment, and airborne dust) by automated single particle SEM/EDX analysis coupled to a machine-learning classifier (described in Järlskog et al., 2022; Rausch et al., 2022), in a rural traffic environment. To the best of our knowledge, the present study is one of the first attempts to characterize, quantify, and differentiate between TWP, bitumen wear particles (BiWP), road marking particles (paint and glass beads), metal particles, and mineral particles in environmental samples and present the results as both relative number- and mass concentrations (%) and as estimations of absolute concentrations. A further and novel aim was to analyze two different size fractions (2–20 μm and 20–125 μm) of samples from all matrices and thereby investigate eventual differences in particle size distribution and particle properties between sample matrices.

2. Method

Samples were collected at Testsite E18, a research station used as a case-study area located on the highway (E18) between Västerås and Enköping, Sweden, Europe (Fig. 1 and Figure S 1). Testsite E18 is located in the central part of Sweden, the climate is mild with an annual mean temperature of 6 °C, (SMHI., 2022a), the road is surrounded by fields, the area is flat, and the yearly precipitation is approximately 700 mm (SMHI., 2022b). The speed limit at Testsite E18 is 120 km/h, and the annual average daily traffic (AADT) is approximately11 000 vehicles (NVDB., 2022). The pavement consists of a stone mastic asphalt with a maximum stone size of 11 mm (SMA11), with polymer-modified bitumen (PMB) as the binder. Testsite E18 has been used as a case study area in previously published studies, both regarding road structures (Rasul et al., 2018), air quality (Svensson et al., 2022), residual salt measurements (Arvidsson et al., 2021), and microplastics and organic pollutants (Dröge and Tromp, 2019). The samples were analyzed with an automated Scanning Electron Microscopy/Energy Dispersive X-ray spectroscopy (SEM/EDX) analytical approach and quantified by a machine learning algorithm as previously described in Järlskog et al., 2022 and Rausch et al., 2022. The samples were categorized into the following subclasses: glass beads, metallic particles, paint particles (Ti-rich, i.e., road markings), bitumen wear particles (BiWP), tire wear particles (TWP), mineral particles, and organic undifferentiated particles (including e.g., pollen, spores, and other organic matter excluding TWP, BiWP and road markings).

2.1. Environmental sampling

The sampling set-up used at Testsite E18 can be seen in Fig. 1 and the sampling dates are shown in Table S 1. Road dust samples were collected in-between the wheeltracks and adjacent to the kerb (named a and b in Fig. 1). Runoff (water and sediment) was collected in the roadside gully pot (named c) and in the stormwater well (named d). To measure the atmospheric transport and deposition of particles from the road, a passive air sampler, named Sigma-2 (VDI2119:2013; Rausch et al. (2022), was placed at the road edge (named e and Figure S 2) and additional Sigma-2 s and deposition buckets were placed at four distances from the road edge (named f). The meteorological data has been collected from the open-source data provided by the Swedish meteorological and hydrological institute, SMHI, and includes precipitation, wind direction, and wind speed (Figure S 3 and Figure S 5) from the national monitoring station in Enköping (59.65 N, 17.12E) (SMHI., 2022a; SMHI., 2022b; SMHI., 2022c). The road is situated in the east-westerly direction and sampling was made south of the road (Fig. 1).

2.1.1. Road dust samples

Road dust samples were collected from the road surface with a Wet Dust Sampler (WDS II). Sampling was performed on five occasions

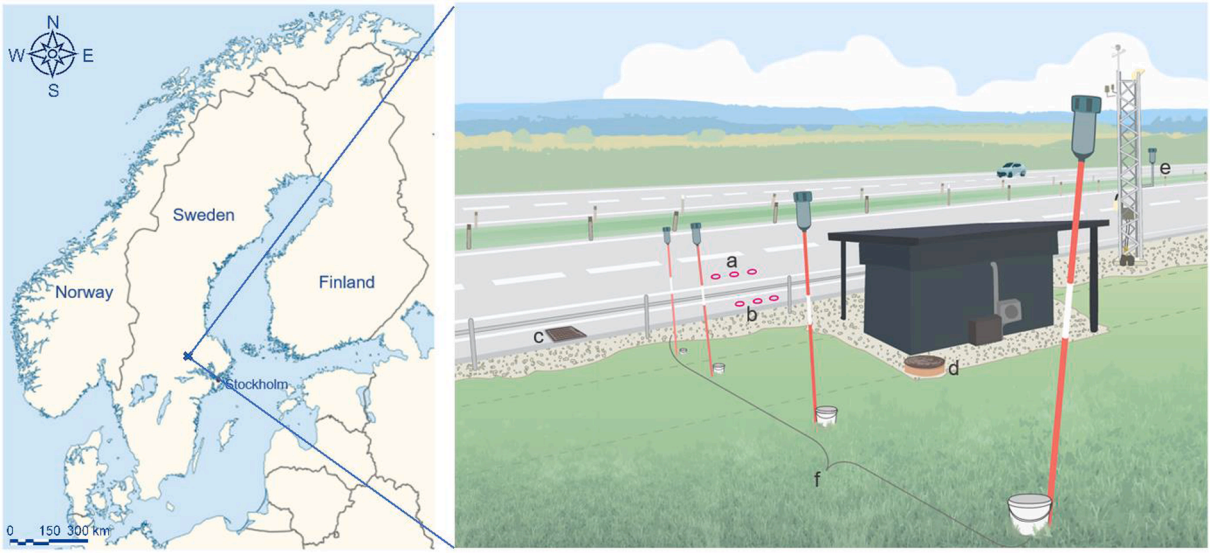

Fig. 1. Left: Location of Testsite E18, 59°38′0.7″N 16°51′12.3″E. Map collected from the Swedish Road Administration and Lantmäteriet, (https://nvdb2012.trafikverket.se) and modified by authors. Right: The illustration shows the sampling spots at Testsite E18; a = road dust samples collected in-between wheeltracks; b = road dust samples collected adjacent to the kerb; c = roadside gully pot; d = stormwater well; e = air sampling placed at the road edge, f = air sampling and deposition buckets at different distances to the road. Illustration: Anna Liljedal.

between 2018 and 2020 to include all seasons (2018–10-04, 2019–06-14, 2020–01-16, 2020–04-08, and 2020–06-04), the precipitation was measured 30 days ahead for each of the five sampling occasions (Figure S 4). WDS II uses a known amount of high pressurized de-ionized water (340 mL) to clean a known area of the road surface (20.4 cm^2). The method has previously been described (e.g., Gustafsson et al., 2019; Jonsson et al., 2008; Järlskog et al., 2022; Lundberg et al., 2019; Rødland et al., 2022b). Each sample bottle contains a composite sample where three WDS II samples have been pooled together (approximately 1 L). Two bottles from each position (kerb and in-between wheeltracks) were analyzed for identification and quantification of traffic-derived particles.

2.1.2. Sediment and water from the roadside gully pot and the stormwater well

Samples were collected on 2020–06-04 and no precipitation had occurred 10 days before sampling. At Testsite E18, all road runoff, collected at a 100 m stretch from are collected in two roadside gully pots and transported to the same stormwater well (through a pipe) (d in Fig. 1). After the stormwater well, the water is released into a ditch and further transported to a small creek without any treatment or cleaning steps. The flow of runoff from the road surface at Testsite E18 starts after 2 mm of precipitation. Water from the roadside gully pot and the stormwater well was grab sampled into 1L glass bottles with a telescopic surface water sampler (similar to the NASCO swing sampler but built at the VTI workshop). Thereafter, sediment was sampled with a tube sampler (Hydro-Bios, Sediment Corer). The amount of precipitation 30 days ahead of the sampling are seen in Figure S 4.

2.1.3. Air and transect samples

Air samples were collected during three periods (January 2020, May 2020, and December 2020) with passive Sigma-2 samplers (following the norm VDI2119:2013) on boron substrates (Figure S 2). Sigma-2 samplers measures the dry deposition as it has a protective cap hindering wet deposition and collect particles in the $PM_{80\text{-}1}$ μm fraction. It is size-selective with an approximate upper cutoff at 80 μm, and a lower cutoff at 1 μm following the sedimentation principle, only particles > 1 μm can be collected quantitatively since smaller particles have a too small sedimentation rate to be sampled passively (Rausch et al., 2022). Sigma-2 s were placed approximately 3.1 m south of the road edge at a height of 2 m above ground level, Figure S 2. The sample from January 2020 was collected for 14 days, the one from May 2020 for 30 days, and the sample from December 2020 for 14 days. In the measurement campaign performed in December 2020, besides the Sigma-2 placed at 3.1 m, samples were collected in a transect on the southern side of the road. Three Sigma-2 samplers were placed at a height of 1.5 m above ground level at different distances (4.8, 27.1, and 100 m) from the road edge to investigate the variation of PM composition and concentrations with distance. To investigate the atmospheric deposition on the ground level, buckets (Ø 17.7 cm) were placed at the same distances from the road as the Sigma-2 s (3.1, 4.8, 27.1, and 100 m) (Fig. 1). The buckets are completely open collecting both dry and wet deposition at all sizes. The buckets are placed on the ground and are more subject to influence of adjacent organic sources (e.g., insect fragments). Few coarse particles depositing in the buckets might influence grain size distribution and hamper comparison between Sigma-2 and bucket sampling. Therefore, this should be done with caution. The total precipitation during the three periods with air measurements was 10 mm (January 2020), 22 mm (May 2020), and 32 mm (December 2020). The accumulated precipitation 30 days before sampling, and during the sampling period are shown in Figure S 4. The wind speed and wind direction during the sampling period can be seen in Figure S 5.

2.2. Sample preparations

Between 2018 and 2020, 19 samples from the road surface, 4 samples from the stormwater well, 4 samples from the roadside gully pot, 6 air samples (Sigma-2), and 3 samples from deposition buckets were collected and analyzed for different traffic-derived particles, Table S 1. A more extensive description of the sample preparation steps can be seen in (Järlskog et al., 2022). A simplified flowchart illustrating the sample collection, sample preparation, particle analysis, classification, and quantification are shown in Fig. 2.

2.2.1. Road dust, sediment, water, and deposition samples

2.2.1.1. Gravimetry. For the gravimetric analysis, 300–500 mL (road dust, water solution, and runoff) and 50 g (wet stormwater and roadside gully pot sediment) were filtered through a pre-weighted Munktell 00*H* filter (particle retention 1–2 μm). The total particle mass (1–2000 μm)

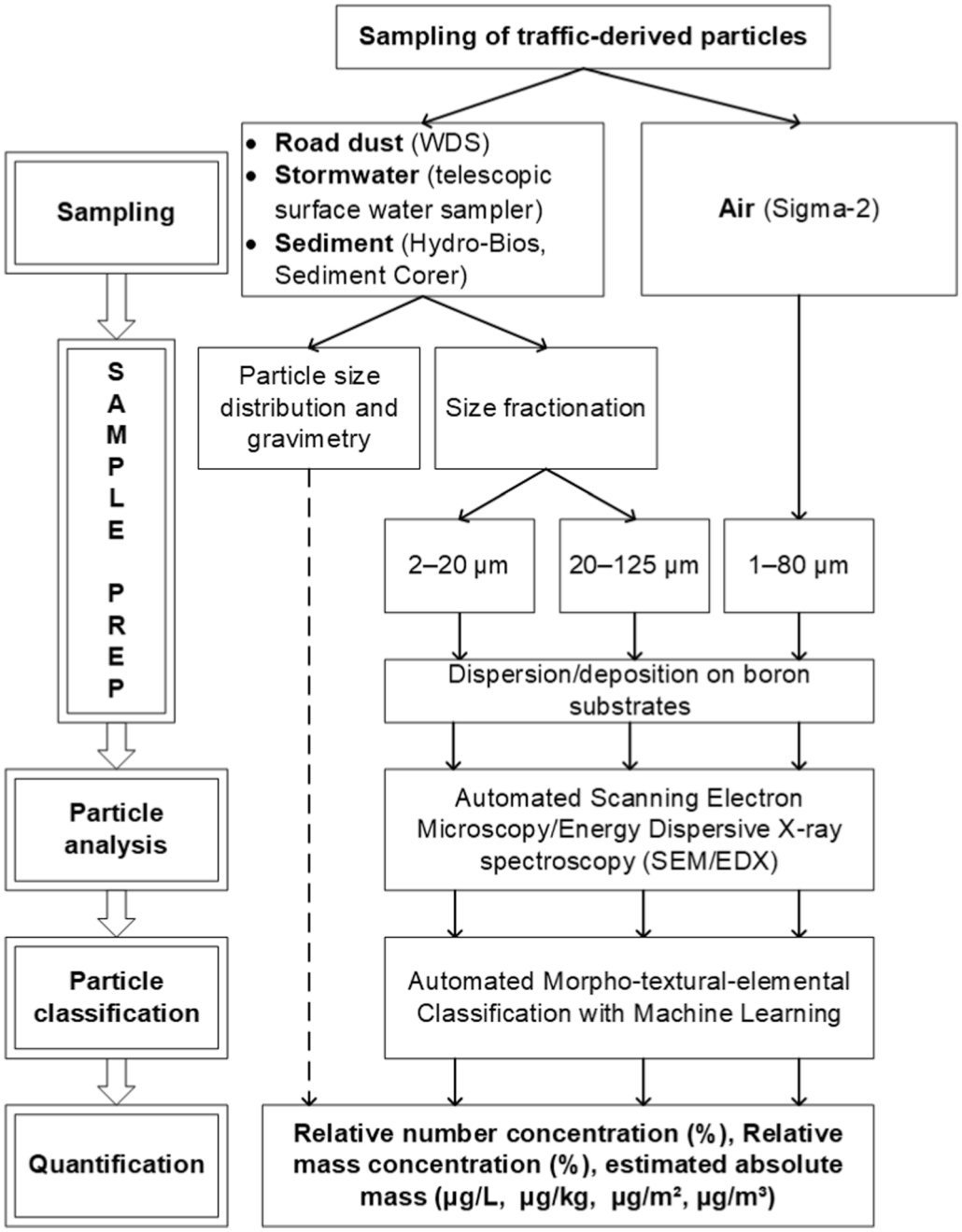

Fig. 2. Schematic figure of the methodology divided into sampling, sample preparation, particle analysis, particle classification, and quantification.

was calculated (g/L). With the results from the gravimetric analysis (g/L) and the area of the WDS II (20.4 cm^2•3), the total amount of road dust was calculated into g/m^2 by assuming that the road dust was evenly distributed on the road surface. The information was used for the calculations of absolute concentrations based on the SEM/EDX data. The transect buckets were weighted and ocular inspected. Since the buckets contained small amounts of material, the samples were diluted with 1 L de-ionized water to enable sample preparation. Of the diluted transect bucket samples 300–500 mL was analyzed for gravimetry. Based on the gravimetry and the area of the bucket (Ø 17.7 cm), the total amount of particles (g/m^2) were calculated assuming that the particles was evenly distributed.

2.2.1.2. Particle size distribution. All samples, except the air samples, were analyzed for particle size distribution (0.125–2000 µm) by laser diffraction (Mastersizer 3000 from Malvern Panalytical). Due to the upper size limit (2 mm) of the laser granulometer, the samples were pre-sieved over an ISO 3310 VWR® 12″ (mesh size 2 mm) and the measurements were performed in triplicates. Approximately 200 mL of the liquid samples (road dust, runoff, and transect buckets) and 50 g of wet sediment were used for the particle size distribution, PSD.

2.2.1.3. Sieving. A known amount (~300 g for road dust samples collected adjacent to the kerb and ~ 500 g for stormwater, transect buckets, and road dust samples collected in-between wheeltracks) were size-fractionated using mesh sieves (VWR test sieves, ISO 3310, 20 and 125 µm) into two size fractions: 20–125 µm and < 20 µm. In the analysis, however, the minimum analyzed size was 2 µm, and the size fraction < 20 µm is hereafter denoted 2–20 µm. For the sediment collected in the roadside gully pot and the stormwater well, representative subsamples

of wet sediment (approximately 50 g each) were taken from the sediment pile, whereafter the subsamples were wet sieved into the same size fractions as the liquid samples (2–20 μm and 20–125 μm). These fractions are in the following text referred to as the finer and the coarser fractions of the samples and should not be confused with the particulate matter (PM) terminology used for airborne particulate matter (e.g., PM_{10} and $PM_{2.5}$). All particles in the two size fractions were transferred onto Whatman Cyclopore Membrane filters (pore size 0.4 μm) and then dispersed on boron substrates using a Morphology G3ID by Malvern disperser (Järlskog et al., 2022) prior to SEM/EDX single particle analysis.

In order to exclude contamination due to the use of tap water, blank samples were prepared using the same methodology, but here 1 L of tap water was sieved and filtered instead of 300–500 mL. Due to the lack of visible particles on the filters, these samples were not dispersed. Instead, the Whatman Cyclopore Membrane filters were coated with carbon and single particle analysis was performed on the filter. The dominant particle group in the blank samples were trace elements, dominated by Fe and Cu. The elemental composition differed from the particles identified in the environmental samples and thus, it can be concluded that the eventual contamination from the sample preparation was negligible (Supplementary material 5.4). Duplicates from all samples (except for the transect buckets due to the small amounts of material) were analyzed to reduce the risk of eventual extreme values from inhomogeneous sample matrices.

To evaluate the potential variation within a sample, and to validate the accuracy of the method, a repeatability test was performed. Five replicates were collected from the same filter, dispersed, analyzed, and classified independently. The results showed that both the relative number- and mass concentrations were similar for all replicates, in both size fractions indicating that the method is reliable and that a subsample can be seen as representative. A more extensive description complemented with boxplots and a table showing particle count, standard deviation, and the relative mass- and number concentrations (%) for each replicate can be seen in the supplementary material (chapter 5.1–5.4, Table S 4, Figure S 12, Figure S 13).

2.2.2. Air samples

Air samples collected on self-made, highly polished boron surfaces (Rausch et al., 2022) did not undergo any further preparation in the lab (i.e., no coating or transfer to another surface). The boron substrates were placed on standard aluminum discs for SEM analysis using a C-pad for fixation and subsequently directly analyzed. This procedure has the advantage of minimizing the chance of contamination of the samples in the lab.

2.3. Analytical method

The samples were analyzed by automated SEM/EDX single particle analysis using a Zeiss Gemini 300 Field Emission Gun (FEG)-SEM equipped with an Oxford X-MAX EDS detector with an 80 mm^2 window, a high efficiency 4 quadrant backscatter electron (BSE) detector and the particle analysis software AZtecFeature (©Oxford Instruments). Particle classification and quantification were performed with a machine learning (ML) algorithm, which makes use of all the available elemental and morpho-textural descriptors (in total 67, 43 determined by the AZtecFeature software and 24 extracted by the ML-algorithm itself) in a "random forest" model trained with>110′000 particles from road samples; The prediction accuracy that is expected from the ML-classifier and further details on the ML-model are shown in Järlskog et al. (2022) and Rausch et al. (2022). The above-described ML-algorithm categorizes the particles into the following subclasses: TWP, bitumen wear particles (BiWP), road markings, reflecting glass beads, metallics, minerals, and biogenic/organics. An extensive method description can be seen in Rausch et al. (2022) and Järlskog et al. (2022). In the finer fraction of the road dust, water, and sediment samples (2–20 μm) it was not possible to satisfactorily differentiate between TWP and BiWP, see further explanation on the differentiation between TWP and BiWP in Järlskog et al. (2022). Therefore, these two subclasses were counted together, hereafter denoted as TBiWP. In the air samples, a differentiation between TWP and BiWP could be satisfactorily achieved for particles $>$ 5 μm owing the pristine appearance of the particles in the airborne Sigma-2 samples. This is partly because these samples do not undergo any sample preparation, and are probably less affected by leaching, alteration, etc., in the environment. However, following a conservative approach, the TWP and BiWP $<$ 5 μm were also summarized in TBiWP as their differentiation towards smaller sizes became also more challenging (Järlskog et al., 2022).

2.4. Estimation of the relative number and mass of particles for the different subclasses

Based on the total number of analyzed particles (average from all road dust and runoff samples, 1223 particles (2–20 μm) and 854 particles (20–125 μm), 527 particles in the air samples $PM_{80\text{-}1}$ μm) and the number of particles classified in the specific subclasses, the relative number concentration of each particle subclass (%) was calculated. To calculate the relative mass concentration, the mass of single particles needs to be estimated. This was done by calculating the volume of a sphere based on the equivalent circular diameter (ECD), i.e., the 2D projection of the particle obtained from the single particle analysis software Aztec Feature (Oxford), and assuming a specific density for each particle group. A density of 1.8 g/cm^3 was used for TWP (corresponding to the average density of the TWP density spectrum shown in Klöckner et al. (2019)), 5.1 g/cm^3 for metallic particles corresponding to the approximate density of hematite, which is by far the most common chemical composition found within the metallic particle group in the analyzed environmental samples, 2.7 g/cm^3 for minerals corresponding to the average density of most common minerals like silicates and carbonates and 1.0 g/cm^3 for biogenic/organic particles as used in Rausch et al. (2022). The density of 1.4 g/cm^3 was assigned to BiWP based on the average TRWP density in Klöckner et al. (2021), 2 g/cm^3 to road marking wear particles corresponding to the average density for thermoplastic road markings in the database of the Nordic certification of road marking materials, NordicCert, and 2.5 g/cm^3 to glass beads (Moghadam et al., 2021). Note that, if needed, the density can be adapted.

2.5. Estimation of the absolute mass and number of particles for the different subclasses

The SEM/EDX analyses were performed on subsamples, meaning that only a small part of the sieved fractions was measured and thus, the total mass cannot be directly determined. This is further complicated by the fact that the samples were divided into two fractions. However, a rough estimation of the total mass and number of particles per subclass can be achieved by using the particle size distributions from the laser granulometer and the information from the gravimetric analysis in combination with the estimated mass per particle and calculated relative mass % per subclass based on the SEM/EDX single particle analysis data as described above. The total gravimetric mass (g/L) of a given sample and the information about the cumulative volume % from the laser granulometer (assuming homogenous density) were used to estimate the share of the mass between 2 and 20 μm and between 20 and 125 μm. The absolute mass and number of the different subclasses was then extrapolated based on the information of the relative mass of the same subclasses within the sieved fractions, Table S 2. In the result section, it was decided to use the estimated absolute masses rather than the estimated absolute numbers. The absolute masses seem to be more representative, especially since the finer fraction (2–20 μm) of road dust contained up to $1.94 \bullet 10^{11}$ TBiWP particles which is unrealistic to count manually.

3. Results and discussions

3.1. Particle size distribution in all matrices

Fig. 3 (left) compares the particle size distributions, PSD, (0.125–2000 μm) from road dust samples (mean values, differences between sample occasions can be seen in Figure S 7) with sediment, and runoff samples collected in the roadside gully pot and from the stormwater well. In the road dust samples, the PSD is broad, with peaks between 20 and 30 μm, similar results have been reported in Järlskog et al. (2020), Klöckner et al. (2021) and Shen et al. (2016). The PSD in the roadside gully pot (both sediment and water) showed a different pattern with a higher proportion of coarse particles, with a median size of 60 μm for water and 100 μm for sediment which is coarser than the average particles in the other sample matrices, but finer than the particles found in roadside gully pot sediment by (Wei et al., 2022) where the average particles were 300–500 μm. The reasons for the coarser particles found in the roadside gully pot can be explained by the fact that particles are transported into the roadside gully pot through runoff. Higher intensity and duration of precipitation enable the transport of coarser fractions of road dust (Xia et al., 2020). When coarse particles reach the roadside gully pot, they settle into the sediment, while finer particles are more easily further transported to the stormwater well. The design of the roadside gully pots and winter maintenance (snow ploughing and grit spreading) can also influence the accumulation of particles (Mengistu et al., 2021; Wei et al., 2022). In the stormwater well (sediment and water), the PSD were finer, with a maximum below 20 μm. A possible explanation for the large number of coarser particles in the roadside gully pot water is that at the moment of sampling, there was pollen floating on the water surface. Under the light microscope it was observed that these samples contained higher amounts of pollen. Due to the overall low concentration of suspended material in these samples a few larger particles can lead to an overestimation of the size in the PSD. Another possibility is that traffic turbulence and the high speed (120 km/h) affects the road dust resuspension (Amato et al., 2017; Le Vern et al., 2021), resulting in an increased deposition in the roadside gully pots. Moreover, road dust has shown hydrophobic properties during sample preparation, which might explain why some large particles remain floating on the water surface (Amato et al., 2013; Bykova et al., 2021).

Particles from the road surface were finer than particles in the roadside gully pot, but coarser than particles from the stormwater well. Particles collected adjacent to the kerb had similar size distributions through all seasons, Figure S 7. For the in-between wheeltrack samples, the sample from January had a broader peak with coarser particles. The in-between wheeltracks samples were slightly coarser than samples collected adjacent to the kerb. A likely explanation is that the finer fractions are depleted from this surface due to intense traffic turbulence, while the kerbside is not exposed to similar resuspension forces. The size distributions of road surface particles are very similar to previously sampled road dust in other road and traffic environments using the WDS (e.g., Gustafsson et al., 2019; Järlskog et al., 2021; Lundberg et al., 2020; Rødland et al., 2022b).

Fig. 3 (right) shows the PSD from the deposition buckets with an average particle size of 30 μm. However, the transect buckets showed bimodal distributions with a second peak towards coarser particles (300 μm), especially prominent for the 4.8 m and the 100 m sample. These peaks are likely caused by single, or few coarser particles deposited into the buckets. At the rather low dust amounts sampled (especially at 100 m), these particles can cause large, but not representative, peaks in a volume distribution. Even if the PSD in the deposition buckets were similar to each other and to the samples from the road surface, the total particle mass showed a clear decrease with distance from the road (13 g/m^2 at 3.1 m, 2 g/m^2 at 100 m) Figure S 8.

3.2. Road dust

3.2.1. Road dust total particle mass (gravimetry)

The total mass of particles (<2000 μm) in the road dust samples collected adjacent to the kerb varied between 400 and 1240 g/m^2 with a maximum during the autumn of 2018 and minimum during the summer of 2019. Independently of season, the other samples (January, April, and June 2020) contained similar total amounts of road dust (approximately 900 g/m^2) (Figure S 6). Similar particle loads (334–1669 g/m^2) were reported from industrial sites in Korea by Jeong et al., (2020), from areas with a high traffic volume in Korea (149–173 g/m^2) (Ha et al., 2012), from urban areas in Mexico City (5.4–173 g/m^2) (Aguilera et al., 2021), and from a tunnel in Norway (6–188 g/m^2) (Rødland et al., 2022b). The similar particle loads are likely to be a result of long-term accumulation of road dust adjacent to the kerb, with relatively small additional accumulation and removal between sampling occasions. For the samples collected in-between wheeltracks, where the dust load is more affected by traffic turbulence, the total amount of particulate matter varied between 2 and 35 g/m^2. The highest concentrations were found in April 2020 and the lowest in June 2019 (Figure S 6). Gustafsson et al. (2019) have shown similar results where the dust load in-between wheeltracks and adjacent to the kerb tends to increase during the spring (studded tires in use) and decrease during summer (no studded tires in use). The

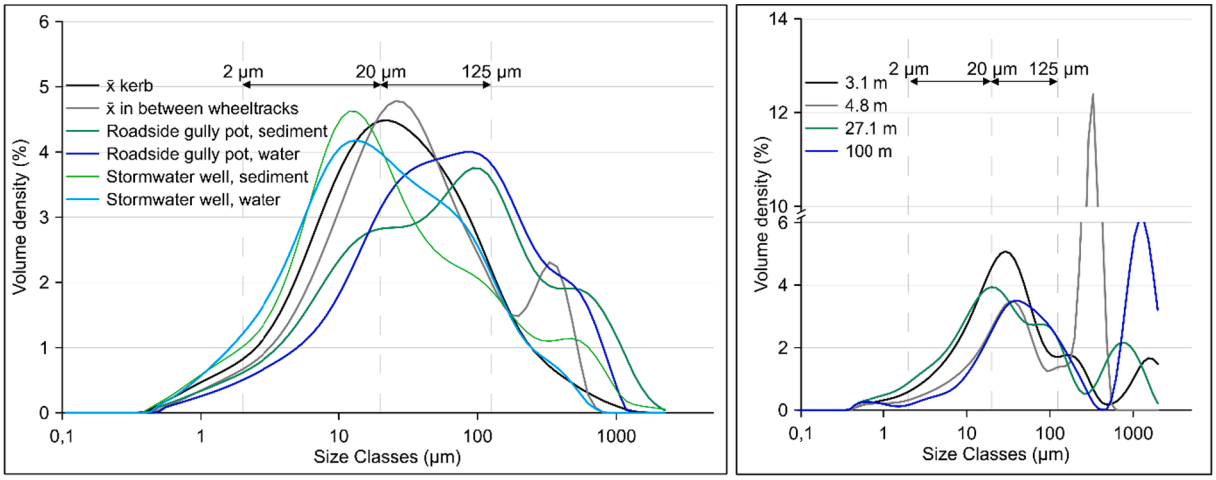

Fig. 3. Particle size distributions. The samples shown in the figure to the left are mean values for the corresponding sample type from all sampling campaigns (kerb, n = 10; in-between wheeltracks, n = 9; roadside gully pot, n = 2; stormwater n = 2). The figure to the right shows the PSD of the deposition bucket samples at different distances from the road edge. The two analyzed size fractions are marked as intervals with arrows.

sampling in June 2019 was preceded by higher, and more recent precipitation (26.9 mm two days before the sampling) than the June 2020 sampling, which could explain the low dust load in June 2019 (Figure S 4).

3.2.2. Road dust composition (relative number concentration in % and seasonality)

The relative number concentration (%) of traffic-derived microplastics and other non-exhaust particles for the road dust collected during the different sampling occasions can be seen in Fig. 4 and Figure S 9. The kerb samples are shown as bright bars and the in-between wheeltrack samples are shown as more faded bars. For the coarser fraction (20–125 μm), a higher relative concentration of TWP was detected adjacent to the kerb compared to in-between wheeltracks (5–22 % and 2–7 %). For BiWP, the relative concentrations were more similar but also higher in kerb samples (3–13 % in the kerb and 2–8 % in in-between wheeltracks). For the finer fraction (2–20 μm), a similar pattern was observed. The relative concentration of TBiWP varied between 11 and 27 % in the kerb samples and 7–19 % in in-between wheeltracks. Rødland et al. (2022b) also found that the highest TWP and BWP concentrations were detected adjacent to the kerb, followed by in-between wheeltracks and Sieber et al. (2020) states that 74 % of the TWP deposits at the roadside. Minerals followed by TWP and BiWP (TBiWP in the finer fraction), are the dominating subclasses in both size fractions and at both positions. The lowest levels of TWP were detected during the sampling in January 2020 (Fig. 4), which is the opposite pattern as the total amount of road dust, Figure S 6, which is higher during the winter period. Moreover, the mineral concentration was higher when TWP was at their lowest levels. The opposite pattern could be seen in the samples from the spring, summer, and autumn, where the mineral concentrations were lower and TWP higher. The sample composition seems to be more affected by the seasonal use of studded tires/summer tires than meteorology. The studs cause more road wear and roughen the road surface while studless winter tires and summer tires polish the road surface. This results in higher generation of TWP during spring when the road surface is rough and tires are switched from studded to summer (Vogelsang et al., 2020).

The sample composition, as well as the particle size distribution is of high relevance to be able to simulate transport of road dust and its components via air and water as the transport depends on both the physical and chemical properties (Fussell et al., 2022). These parameters are also relevant with regard to the potential health and environmental impacts of the road dust during different seasons.

3.2.3. Road dust composition, estimated absolute mass

Based on the results from the gravimetry, the PSD, and the SEM/EDX/machine learning differentiation, an estimated absolute mass (g/m^2) was calculated, Fig. 5 and Figure S 10. The results showed that the estimated mass of traffic-derived microplastics in the coarser fraction varied between 3 g/m^2 (January) to 43 g/m^2 (October) for the TWP, and between 10 g/m^2 (June) and 25 g/m^2 (January) for the BiWP in the kerb samples. The amount of TWP in-between wheeltracks was substantially lower, 0.01 g/m^2 (October) and 0.2 g/m^2 (April), for the BiWP, the estimated masses varied between 0.04 g/m^2 (June) to 0.3 g/m^2 (April). The seasonal variations between TWP and BiWP can also be explained by the use of studded tires (Vogelsang et al., 2020). This is important to consider in forth-coming studies based on field measurements. For example, for pollution transport modelling and risk assessments, especially since the relative number concentration (%) of TWP were similar between the two positions. As an example, the average TBiWP mass (both size fractions) in samples collected adjacent to the kerb was 85 g/m^2. This value is ten times higher than the average mass in in-between wheeltrack samples (0.8 g/m^2). In another WDS study, where road dust samples were collected at different positions in a tunnel in Norway, the TWP concentrations varied between 0.025 and 4.8 g/m^2, and the highest concentrations were detected adjacent to the kerb (Rødland et al., 2022b, Figure S 13). Highways in Sweden are rarely swept, thus the road dust collected adjacent to the kerb can accumulate for a long period. That might explain the large deviations between the kerb and in-between wheeltracks. Therefore, it is probably more realistic to see the accumulation at the kerb as a storage location and assume that the material can be further transported during heavy rains and windy episodes (Wang et al., 2022). The results further showed that both absolute and relative estimates provide the same pattern with minerals as the most common subclass followed by TWP and BiWP (Figure S 10, Fig. 5).

3.3. Sediment and water (roadside gully pot and stormwater well)

3.3.1. Sediment and water total particle mass (gravimetry)

The gravimetric analysis of the water samples showed that the particle mass in the water was almost six times higher in the stormwater well compared to the roadside gully pot (1.1 g/L vs 0.2 g/L). The PSD indicates that the particles in the roadside gully pot, both for water and sediment, were coarser than in the stormwater well, as also mentioned in 3.1 and Fig. 3. A reason for the lower particle mass in the roadside gully pot water is that the particles have either sedimented or have been further transported downstream instead of remaining floating in the roadside gully pot water. Large amounts of precipitation occurred 12 and 22 days prior the sampling (figure S 3 and S 4). Those rain events

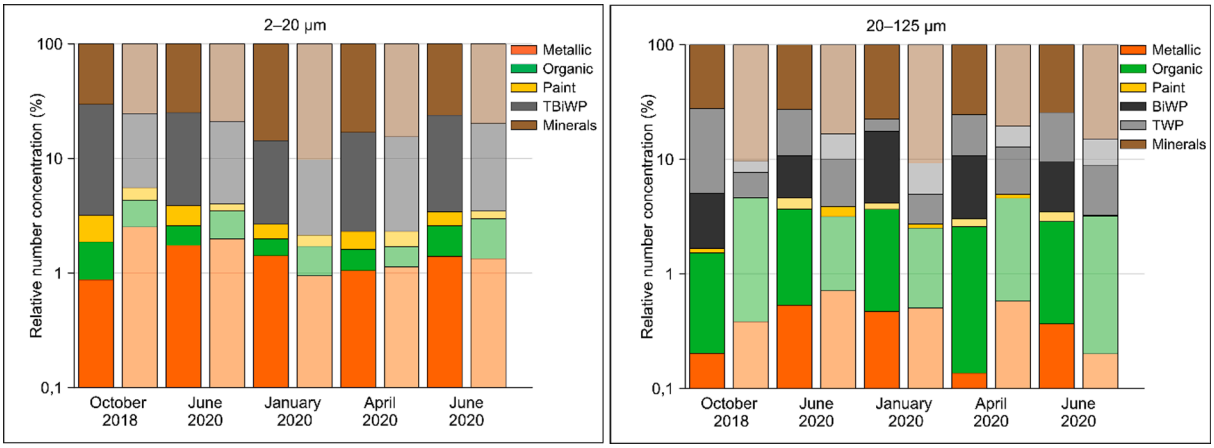

Fig. 4. Comparisons of relative number concentration (%) for particles collected adjacent to the kerb (bright color bars) and in-between the wheeltracks (faded color bars) divided into the different subclasses. The results of the finer fraction (2–20 μm) are shown in the left side, while the results of the coarser fraction (20–125 μm) in the right side. The bars are mean values of the duplicates analyzed for each of the five sampling occasions. Note that the bars are logarithmic.

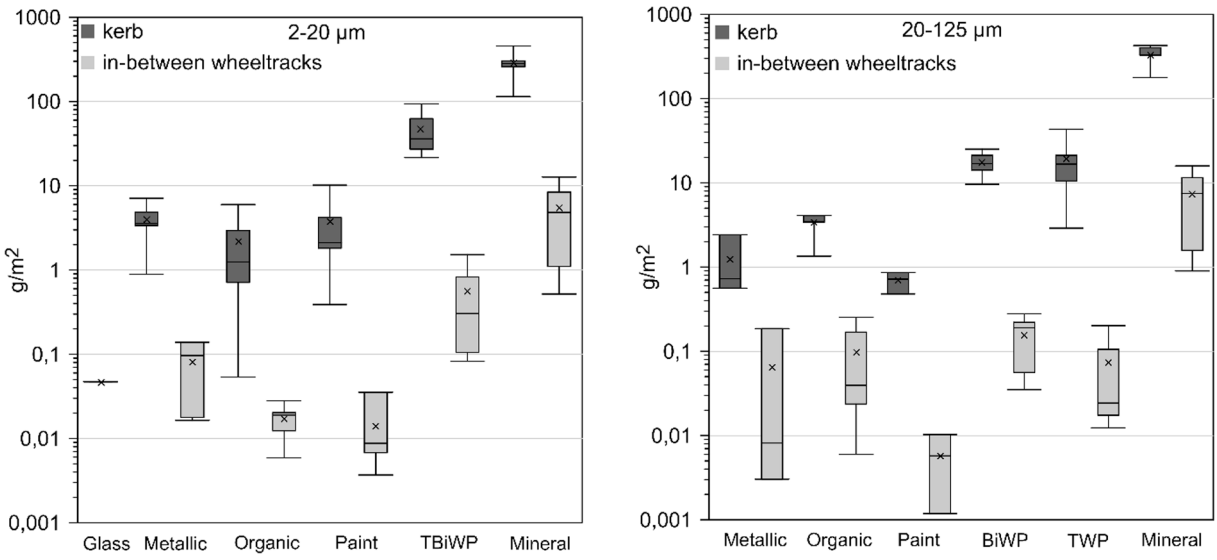

Fig. 5. Comparisons of the estimated mass (g/m^2) for the road dust samples. Kerb samples (n = 10) are shown in dark boxplots, and in-between wheeltracks samples (n = 9) are shown in the light boxplots. The mean value is shown with a cross and the median with a line through the boxes. The edges of each boxplot represent the quartiles, and the whiskers show the 10 and 90 percentiles. The results of the finer fraction (2–20 µm) are shown on the left side, while the results of the coarser fraction (20–125 µm) in the right side.

probably transported some of the particles from the roadside gully pot further to the stormwater well. After high particle concentrations in the first flush during a rain event, the run-off water has lower particle concentrations. The high dust load of the first flush will be transported further downstream to the run-off well, while the gully-pot will successively receive less dust laden run-off water. Also, the small volume of the gully pot favors higher flows, resulting in coarser and heavier particles remaining in the gully pot. A small rain event (<2 mm) occurred 7 days before sampling, but was too small to cause any runoff.

3.3.2. Sediment and water composition (relative number concentration in %)

3.3.2.1. Runoff water. The relative number concentrations (%) of the different subclasses differed between the roadside gully pot and the stormwater well (Table S 2 and Figure S 9). In the coarser fraction (20–125 µm) from the roadside gully pot, the relative concentration of traffic-derived microplastics, i.e., TWP was 25 % and of BiWP 6 %, while the stormwater well contained 35 % of TWP and 3.5 % of BiWP. A higher amount of minerals was detected in the roadside gully pot (65 % compared to 54 % in the stormwater well). Another noticeable difference was that more organic material was detected in the stormwater well (7.5 %) than in the roadside gully pot (2.5 %). For the finer fraction (2–20 µm), 43 % of TBiWP were detected in the roadside gully pot, and 31 % in the stormwater well, which is the opposite pattern compared to the coarser fraction. Even the mineral concentration was lower in the roadside gully pot (43 %) compared to the stormwater well (64 %). This result indicates that the finer mineral particles are transported to a greater extent than the coarser particles, as expected.

3.3.2.2. Runoff sediment. On the contrary, a lower percentage of TWP was found in the coarser fraction of the sediment in both the roadside gully pot and the stormwater well compared to the water phase., see Table S 2, Fig. 10, and Figure S 9. The result can be explained by the lack of heavy precipitation prior to the sampling date since the intensity of the rainfall is directly related to the number of particles floating in the water (Xia et al., 2020), resulting in sedimentation of coarser particles. The coarser fraction (20–125 µm) of the roadside gully pot sediment contained 13 % of TWP, 11 % of BiWP, and 70 % of minerals. For the stormwater well sediment, 24 % consisted of TWP, 12 % of BiWP, and 57 % of minerals. In the finer fraction (2–20 µm), the relative concentration of TBiWP in both the roadside gully pot and the stormwater sediment was very similar. This indicates that the stormwater system might be the major transportation route of TWP as previously stated by e.g., Wang et al. (2022).

Compared to samples collected on the road surface, the relative number concentration of TWP (both size fractions) was higher in the water and the sediment in both the stormwater well and the roadside gully pot. A possible explanation is the occurrence of a higher proportion of larger and heavier mineral particles in samples collected at the road surface, i.e., closer to the source. The road dust accumulates at the kerb for a long time, especially during a period with little precipitation and low wind speeds. In these meteorological conditions, the road dust generated is not removed by runoff and will therefore accumulate. Moreover, lighter particles like TWP will be more easily transported by runoff, which would cause a higher proportion of TWP in the runoff dust load than in the remaining on-road dust load.

3.3.3. Sediment and water composition (estimated absolute mass concentration)

The calculated masses in water and sediment are presented in Fig. 6 and Table S 2. In the coarser fraction of the roadside gully pot sediment, 3.5 g TWP/kg and 9.3 g BiWP/kg were detected. In the stormwater sediment, 14.5 g TWP/kg and 26.5 g BiWP/kg were found. The finer fraction of the sediments contained 21.4 g TBiWP/kg (roadside gully pot) and 71 g TBiWP/kg (stormwater). Rødland et al. (2022b) found 3–54 g TWP/kg (median 7 g/kg) and 2.4–43 g polymer modified bitumen (PMB)/kg (median 5.2 g/kg) in sediments from roadside gully pots located in a tunnel in Norway. The samples were analyzed with a novel pyr-GC/MS method that enabled the estimation of the amounts of TWP, and PMB. The lowest concentrations were found in the roadside gully pot located in the middle of the tunnel, and the highest concentrations were from the gully pot at the inlet of the tunnel. The results of the present study were in the same concentration range as those in Rødland et al. (2022b). The results from the present study are also well in line with a previous study by Mengistu et al. (2021) where the authors analyzed gully pot sediment and concludes that up to 1–150 g/kg of the sample consists of TWP (Figure S 14). The stormwater well also contained a higher content of organic/biogenic material compared to the roadside gully pot. The roadside gully pot water contained 0.01 g/ TWP/

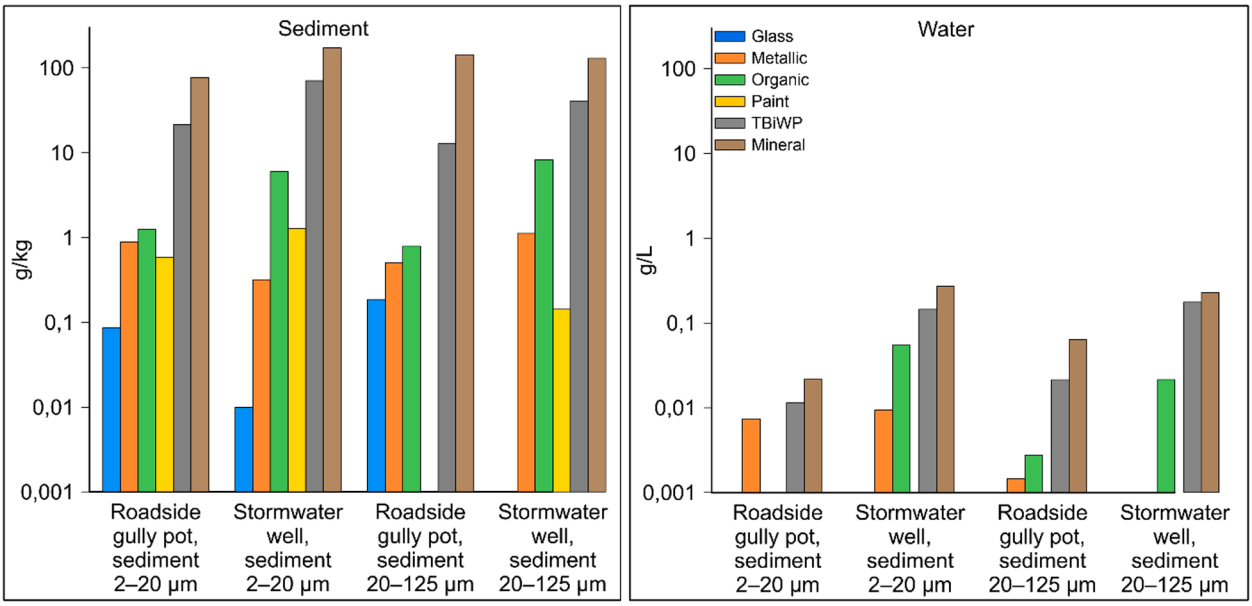

Fig. 6. Estimated mass (g/kg and g/L) for sediment and water samples collected in the roadside gully pot and the stormwater well. The results of the sediment samples are shown to the left, while the ones of the water samples to the right.

kg in the coarse fraction and 0.01 g TBiWP/kg in the finer fraction while the stormwater contained 0.13 g TWP/L in the coarser fraction and 0,15 g TBiWP/L in the finer fraction. The results from the stormwater are within the same order of magnitude as previously published studies e.g., Parker-Jurd et al., (2021) (>15 µm, 0.0025 g/L), Kumata et al., (2002) (0.0006–0.179 g/L) even though different analytical methods, sampling techniques, and size ranges has been analyzed. The findings from this study confirms previous findings e.g., Wang et al. (2022), that the stormwater system is an important transport route for traffic-derived microplastics especially since the main part of road runoff from highways (and rural areas) is not treated prior to release into the environment.

3.4. Airborne dust (mass concentration and deposition)

3.4.1. Composition of airborne dust $PM_{80\text{-}1}$ (mass concentration)

As in the road dust samples and the runoff samples, the air samples are dominated by minerals (11.9–16.3 µg/m^3) followed by biogenic/organic particles (1.1–6.2 µg/m^3), traffic-derived microplastics, TWP > 5 µm (1.4–2.4 µg/m^3), BiWP > 5 µm (0.3–0.9 µg/m^3), metallic wear particles (0.1–0.9 µg/m^3), and with the lowest concentrations, paint wear particles (0.02–0.1 µg/m^3), note that the air was analyzed in the $PM_{80\text{-}1}$ fraction as previously mentioned in 2.1.3. TWP always occur in higher concentrations than BiWP (Fig. 7). The TBiWP fraction comprising TWP and BiWP particles < 5 µm that could not be unambiguously differentiated into the two subclasses separately, amounts to 0.3–0.8 µg/m^3. This underlines the abundance of tire and bitumen particles also in the airborne inhalable particle fraction. Recently published studies based on field measurements of TWP reports

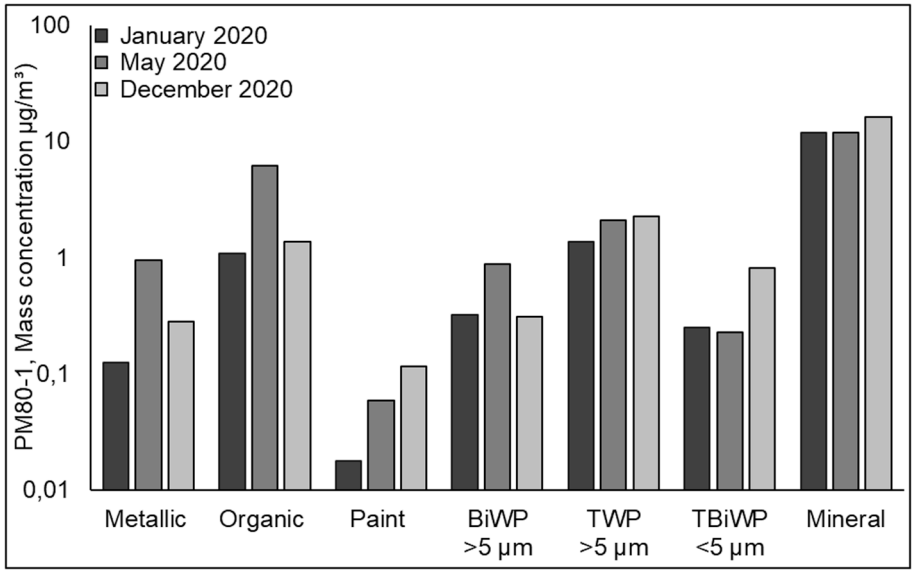

Fig. 7. Comparison of air samples collected with the Sigma-2 passive sampler (VDI2118:2013) 1.5 m from the road edge during three different periods of the year. The mass concentration in µg/m^3 of the different particle subclasses within $PM_{80\text{-}1}$ is shown.

concentrations in the air at busy roads in Denmark (2.81 μg/m^3) (Fauser et al., 1999) and Spain (3.4 μg/m^3) (Amato et al., 2014), at urban sites in the US (0.2–2 μg/m^3) (Schauer et al., 2002), and at ambient air in Germany and Switzerland varying between 0.2 and 0.5 μg/m^3 and 2.17 μg/m^3 (Fomba et al., 2018; Rausch et al., 2022). The studies have used different methods for sampling, sample preparation, and analyses (including different settings on the instrument, and various markers for identification of TWP. However, the results are within the same size range as the present study, (Figure S 14). Metallic particles, most likely largely derived from brake wear, also play an important role in all air samples with concentrations ranging between 0.1 and 0.9 μg/m^3. Paint wear particles occur in significantly lower concentrations (0.02–0.1 μg/m^3) but are also present in the three airborne dust samples.

3.4.2. Variations in airborne samples due to seasonality and meteorology

In May 2020, the concentrations of bitumen wear particles were almost three times higher than in the winter samples. That can be explained by the increased generation and accumulation of bitumen particles during the previous months due to the use of studded tires, in combination with warmer and drier conditions promoting road dust resuspension (Gustafsson et al., 2019). The amount of precipitation was higher in December and January compared to in May. In general, the colder and more humid weather during the winter often results in moist road surfaces which allows particles to be trapped at the road surface rather than to be transported into the air (Denby et al., 2013). During the winter, the vehicle speed is often lower due to snow and ice cover which can also reduce the turbulence and resuspension of particles by traffic. The wind speed was higher during the winter and the wind direction varied compared to the May sampling campaign, (figure S 3. S 4, S 5), meaning that the particles that were released into the air were transported further away from the road with a higher speed than the particles in May. Moreover, the sampling in May occurred for 30 days compared to 14 days for the respective winter sampling campaigns (January and December). Further, the mass concentration of $PM_{80\text{-}1}$ biogenic/organic particles is relatively high and variable upon season ranging between 1.1 and 6.2 μg/m^3. The biogenic/organic mass concentration was almost six times higher in May 2020 compared to the winter samples from January 2020 and December 2020 (Fig. 7). The high concentration in May reflects the typical increased biological activity during the spring season (and also summer), which is responsible for the enhanced emission of natural particulate matter like pollen and spores and secondary organic compounds (Gelencsér et al., 2007; Li et al., 2021; Yttri et al., 2019).

Factors like turbulence and mixing height (determined by temperature gradient), wind speed, wind direction, and precipitation during the sampling periods may impact the concentrations found in the air samples (Fussell et al., 2022; Klein and Fischer, 2019; Xia et al., 2020). During the measurement period in May 2020, the dominant wind direction (was crosswise from the road (north) towards the sampling point (south), while in January and December 2020, the dominant wind directions were southwest and southeast, respectively (Figure S 5). This had most likely the effect of diluting the contribution of road/traffic-derived particles and incrementing the concentration of particles derived from other sources located southwest (agricultural fields), resp. southeast (agricultural fields), in the collected air samples. The predominant N—S wind direction during May 2020 is likely to have exerted an influence on the higher mass concentration of BiWP, metallic, and biogenic/organic particles during that measurement campaign. Further, the last precipitation preceding and during the sampling occasions varied (Figure S 4) with 26 mm 30 days before and 21.6 mm during the measurement in May 2020, while the precipitation before the sampling occasions in January and December 2020 were higher (47 mm and 73 mm respectively). During the winter period, the road surface is often moist, and the particles tend to stay longer on the road surface than during the spring and summer when the road surface dries up more quickly due to higher temperatures (Denby et al., 2013). Even though biogenic/organic particles play a worth-mentioning role (in average 12 % of $PM_{80\text{-}1}$, Fig. 10) in the PM composition of the studied airborne samples, it is still obvious that the airborne dust at the studied site is dominated by traffic-related emissions (minerals, BiWP and paint wear particles from road wear, TWP and metal wear from tire and brake abrasion, respectively). This is the case for all studied seasons.

3.4.3. Variations in mass concentration of airborne particles with increasing distance to the road (Sigma-2 transect measurement)

The results from the transect using Sigma-2 passive samplers (placed at 4.8 m, 27.1 m, and 100 m from the road edge) shows that the highest concentration of particles was found in the sampler closest to the road. And the concentration decreased with increasing distance to the road for all subclasses except for the organic/biogenic, which increased at 27.1 m compared to 4.8 m (Fig. 8 and Figure S 11). This is in agreement with a previous study by Sommer et al. (2018), where traffic-derived non-exhaust particulate matter in super-coarse (i.e., PM_{80-10}) air samples (4.6 m from the road) were dominated by traffic-derived abrasion (89 %) of which 33 % were TWP. In this study, as in the study by Sommer et al. (2018), the results indicate that the majority of the particles in the air (except for the organic/biogenic) could be related to traffic.

3.4.4. Variations in atmospheric deposition of airborne particles with increasing distance to the road (bucket transect measurement)

The gravimetric results from the deposition buckets showed that the total mass of particles (g/m^2) decreased with increasing distance to the road (13 g/m^2 at 3.1 m; 5.6 g/m^2 at 4.8 m, 6.4 g/m^2 at 27.1 m, and 2 g/m^2 at 100 m), except for the deposition bucket placed at 27.1 m which contained approximately 1 g more particles/m^2 (Figure S 8). The increased particle load at 27.1 m can be explained by the higher concentration of organic material in that bucket. The particle load was estimated based on the results from the gravimetry, the area of the bucket opening, and the assumption that the particles were evenly deposited on a square meter. Due to the low number of particles that were deposited in the buckets, it was judged that it is more reasonable to use the relative mass concentrations (%) instead of relative number concentrations (%) for the discussion of these results. As seen in Fig. 9, the majority of the particles, even at longer distances, can be related to traffic. The meteorological data indicates that even if the wind speed was low during the measurement period (December 2020), no inversion occurred, the predicted turbulence was low, and the dominant wind direction was towards the deposition buckets (Figure S 5). This, and that the concentrations of TWP is reduced away from the road, is also in agreement with previous findings of traffic-related particles (Mori et al., 2018) and recently TWP findings by Parker-Jurd et al. (2021) and Goβmann et al. (2021).Further, particulates suspended in the atmosphere might removed by wet deposition (Wright et al., 2020) which could result in higher concentrations of traffic-derived particles even at more remote distances from the road.

3.5. Distribution of traffic-derived particles in different environmental compartments

A schematic illustration of transport routes and dispersal pathways of traffic-derived microplastics and other road related particulate matter at Testsite E18 (Sweden) is shown in Fig. 10. The specific numbers presented in the figure will vary from site to site depending on the vehicle volume and road configuration. The principal transport mechanisms and pathways, however, might be applicable to traffic environments in general. The particles are generated at the road surface, and thereafter either transported into the environment directly through the air and deposited down-wind of the road or deposited at the road surface as a dust load. The dust load is then either transported during precipitation events through road runoff or splash and spray, resuspended in the air, accumulated at the road edge, or infiltrated in the ditches. The results have been summarized in pie charts showing the relative number concentration (%) (for road dust and runoff) and relative mass

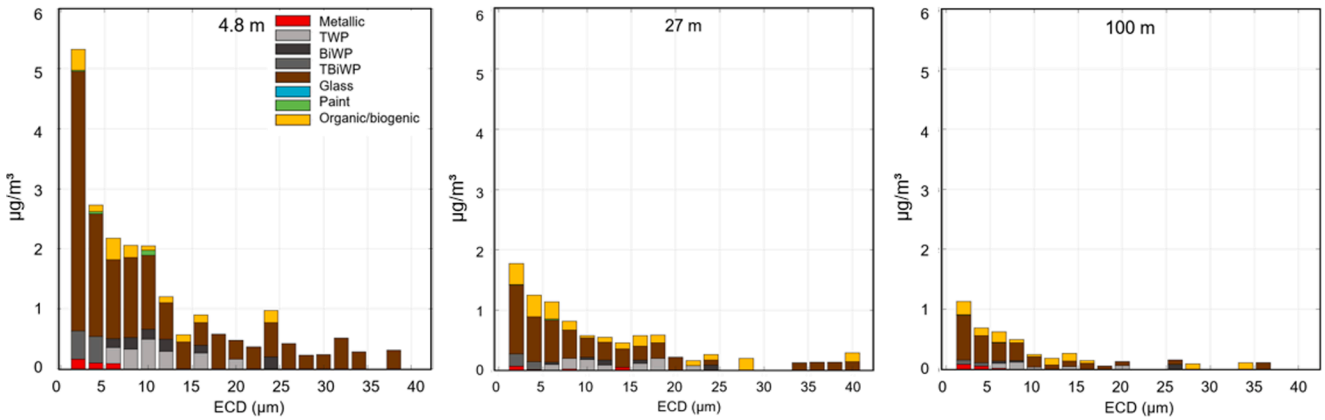

Fig. 8. Comparison of size-resolved mass concentrations ug/m^3 of the differentiated particle subclasses within the samples collected with Sigma-2 samplers in a transect with samplers installed at 4.8 m, 27.1 m, and 100 m from the road edge. ECD = Equivalent Circular Diameter.

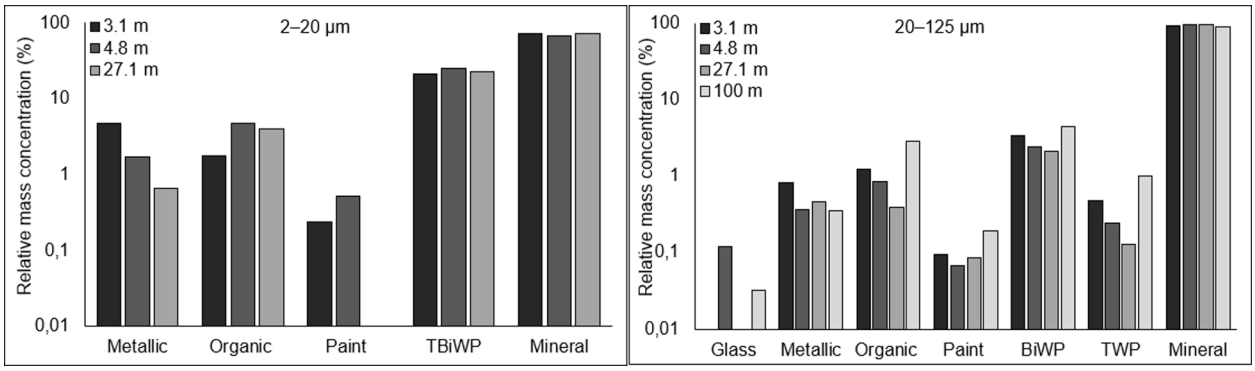

Fig. 9. Relative mass concentrations in percentage of the different particle subclasses as a result of atmospheric wet and dry deposition into buckets at different distances from the road edge. See Figure S 8 for absolute deposition into buckets.

concentration (%) (for air and deposition) of glass fragments from reflecting glass beads, metallic particles mainly from break wear, biogenic/organic particles mainly from nature, road marking paint wear, TBiWP, and minerals for the different environmental compartments (mean values of the entire size fractions analyzed for the different sample matrices). The calculated absolute masses (see section 2.5.) can be seen adjacent to the respective pie chart (Note that the absolute masses are presented with different units).

The relative number concentration (%) of TBiWP was highest in the roadside gully pot water (38 %) followed by the water in the stormwater well (34 %), sediment in the stormwater well (33 %), roadside gully pot sediment (26 %), road dust from the kerb (20 %), road dust from in-between the wheeltracks (12 %), and finally in the air samples, both from the atmospheric deposition buckets (12 %) and airborne $PM_{80\text{-}1}$ Sigma-2 samples (4 %). The same pattern was detected in both size fractions (2–20 µm and 20–125 µm), Table S 2, and can partly be related to precipitation, wind speed, and wind direction. The share of TBiWP was lower closer to the source (i.e., at the road surface), likely due to the higher content of heavier mineral particles, largely stemming from road abrasion, closer to the source. The mineral particles sediment to a higher extent in the ditch or adjacent to the kerb, increasing the relative content of TBiWP further away from the road surface. The results from the calculations of absolute masses showed that for the solid samples, the highest concentrations of TBiWP were found in the stormwater sediment (112 g TBiWP/kg). The roadside gully pot sediment contained much lower TBiWP masses (34 g TBiWP/kg). Samples collected adjacent to the kerb had much higher concentrations (85 g TBiWP/m^2) than the samples from in-between wheeltracks (0.8 g TBiWP /m^2) which partly is a result of the dominating wind speed and wind directions, but also from turbulence from the traffic and precipitation (Gustafsson et al., 2019; Xia et al., 2020). For the water samples, the roadside gully pot had ten times lower concentrations (0.03 g TBiWP /L) than water in the stormwater well (0.3 g TBiWP /L), indicating that the total number of particles were higher in the stormwater well compared to the roadside gully pot. The air contained 3 µg/m^3 of TBiWP in the size fraction $PM_{80\text{-}1}$ and 0.8 µg/m^3 of TBiWP in $PM_{10\text{-}2.5}$, which is in-between the values reported in Rausch et al. (2022) for a traffic and an urban background site. These results suggest that measures to reduce the amount of TWP and BiWP for further spreading should be focused to the kerb, and when it is possible, to sediment and water of the stormwater wells.

Another important finding is that the estimated masses in the sediment were higher for the finer fraction than for the coarser fraction. Sediment from the stormwater well consisted of 70 g TBiWP/L in the finer fraction and 41 g TBiWP/L in the coarser fraction. For the roadside gully pot, 21 g TBiWP/L were detected in the finer fraction compared to 13 g TBiWP/L in the coarser fraction, Fig. 6. The same pattern was detected for road dust (Fig. 5). Previous literature has sometimes excluded finer particles from the analyses, and it has been discussed that finer particles (<20 µm) doesn't have significant contribution to the total mass. This result clearly shows the opposite, and it should encourage to include the finer fractions (i.e., < 20 µm) in the forthcoming studies.

3.6. *Strengths, limitations, and potential further work*

The sampling (WDS II, Sigma-2) and analytical (automated SEM/EDX single particle analysis coupled to an ML-based classification) method used in the present study was able to recognize, differentiate,

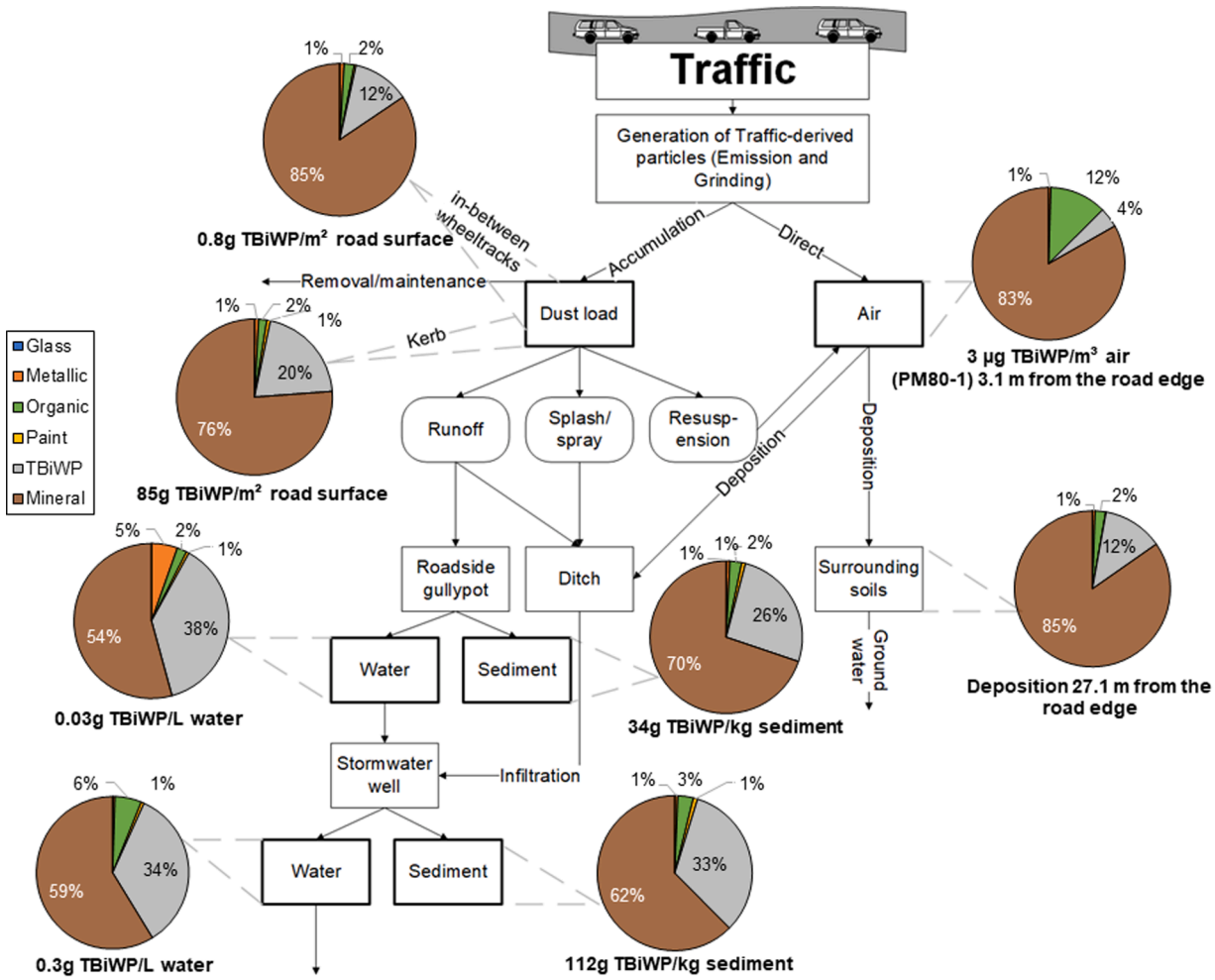

Fig. 10. The main dispersion routes of traffic-derived particles at Testsite E18 combined with the results presented as relative number concentration (%) (relative mass concentration (%) for air) and absolute mass of TBiWP from samples collected in the different matrices (therefore displayed in different units). The subclasses TWP and BiWP are counted together, and the size fractions (2–20 µm and 20–125 µm) have been combined. The pie charts show the mean values of the relative number concentration (relative mass concentration for air) for each sample matrix and the absolute mass is an average.

and quantify between various subclasses of traffic-derived microplastics (TWP, BiWP, and road marking paint) and other non-exhaust particles (minerals, metallic and glass beads) in a variety of sample matrices. The relative number concentration enabled comparisons between different sample matrices while the estimated absolute masses enabled rough comparisons between previously published studies. In addition, the SEM/EDX-ML approach provides information about morphological parameters, like size, shape, and texture of the particle surfaces, which are of importance to increase the knowledge on aging, deposition, and transport of the particles.

Uncertainties of the applied methodology include the conversion of 2D particle projections to 3D volumes and the attribution of specific densities to the particles based on the assigned subclass (e.g., 1.8 g/cm^3 for TWP). The influence of these uncertainties in the quantifications has been previously discussed by Rausch et al. (2022).

A limitation of the used methodology is that samples (except for airborne, Sigma-2) needed to be divided into two fractions. The reason why this step was necessary lies in the fact that it is unpracticable to analyze the complete size range (2–125 µm) by SEM/EDX single particle analysis in a single analytical run. To guarantee statistically significant results for both the fine and the coarse particles, a very large number of particles, and therefore, an extremely long analytical time would be necessary. Therefore, under the actual analytical possibilities, this was considered unrealistic, especially in view of the large number of samples investigated in this study.

The passive air sampling performed with Sigma-2 s has an upper cutoff of around 80 µm and a lower cutoff of around 1 µm. A drawback of the passive sampling method is that particles < 1 µm cannot be collected and analyzed quantitatively since particles finer than 1 µm have a too small sedimentation rate to be sampled passively. A possible solution could be to use active samplers for forthcoming studies. However, an active sampler requires electricity and a more work intense operation. Further, boron substrates are not suitable for active samplers, and the use of conventional filters (e.g., made of polycarbonate) is not suitable for the analysis of traffic-derived carbonaceous particles with SEM/EDX for the following reason: these filters contain carbon, thus, the quantification of carbon on a carbon-bearing filter is not possible. However, the element carbon is of importance for the differentiation between particle subclasses and the automated classification, meaning that the lack of carbon as a diagnostic criterion would deteriorate the results. Therefore, at the moment, the classification of particles < 1 µm is too challenging.

A suggestion for upcoming studies is that multiple analytical strategies are used, e.g., the automated SEM/EDX in combination with pyr-GC/MS to be able to compare results obtained from intrinsically different but probably complementary methodologies. For future work, additionally, it would be of interest to collect more samples from the roadside gully pots and the stormwater well, preferably in all seasons, to investigate potential meteorological differences. More detailed sampling before, during, and after a rain event could be used to better understand

particle transport in the different parts of the system and how it affects the composition and size distributions. It could also be of interest to perform additional analyses to quantify metals, organic pollutants, and other microplastics to further increase the understanding of the sample composition.

4. Conclusions

This study investigated the occurrence and concentrations of traffic-derived microplastics and other non-exhaust particles in various sample matrices close to a rural road environment, with a special focus on TWP and TBiWP. The results confirm previous findings that TWP are an important source of microplastics and indicate that large amounts of TWP are transported from the road surface into the stormwater and air, but also that the samples closer to the source (i.e., road surface) contain more heavy particles (i.e., minerals) than samples collected at longer distances.

The particle size distribution highlighted the importance to include the finer fractions in the investigations since the average particle size varied between 10 and 100 μm independent of sample matrix and the estimated absolute masses showed that the finer fraction (2–20 μm) corresponds to>50 % of the TBiWP (mass) in samples from all matrices indicating that the finer fraction is more important than previously reported. Moreover, the 2–20 μm fraction dominated (both by mass, volume, and number) in all sample matrices. This is an important finding since finer particles have a high potential to be transported in water and air far away from the source and parts of the 2–20 μm fraction can also contribute to the inhalable particle fraction (PM_{10}) in air. The total particle mass reduced drastically with an increased distance from the emission source. However, with time, the accumulated loads of traffic-derived microplastics and non-exhaust particles within stormwater and surfaces affected by atmospheric deposition of airborne dust may become high also at distant recipients.

The highest share (relative number concentration %) of TWP and TBiWP was found in the water from the runoff (roadside gully pot and stormwater well), with a mean number concentration of 37 % in the 2–20 μm fraction and 30 % in the 20–125 μm fraction. At the road surface, the average number concentration proportions were 19 % (kerb) and 14 % (in-between wheeltracks) in the 2–20 μm fraction, and 15 % (kerb) and 6 % (in-between wheeltracks) in the 20–125 μm fraction. On the other hand, the estimated absolute masses showed that the TBiWP were higher in the sediment collected in the stormwater well (70 g TBiWP/kg (2–20 μm) and 42 g TBiWP/kg (20–125 μm)) than in samples collected adjacent to the kerb (48 g TBiWP/kg (2–20 μm) and 36 g TBiWP/kg (20–125 μm)). Further, a seasonal increase of BiWP was observed in the coarser fraction (20–125 μm) of the kerb samples during winter, most likely reflecting studded tire use.

Even though the Sigma-2 airborne and the deposition bucket samples contain the lowest relative mass concentrations of TBiWP compared to the other environmental compartments, they still consist of a considerable share of these particles (4 % and 12 %, respectively). It is especially of relevance when considering the distal paths that small particles can travel under certain atmospheric processes (e.g., mineral particles transported large distances during Saharan dust events), and their potential accumulation on surfaces like agricultural soils through atmospheric deposition over time.

The findings from this study indicate that the stormwater system is an important transport route of TWP and other traffic-derived particles especially since the main part of road runoff from highways (and rural areas) is not treated prior to release into the environment. The results also confirm that the road dust contains large amounts of traffic-derived microplastics meaning that measures should be implemented to prevent further transport into the environment. A comparison of our results with other previous published studies, shows that they are within the same concentration range, suggesting that the concentrations of TWP In different sample matrices are similar on a global scale.

Declaration of Competing Interest

The authors declare that they have no known competing financial interests or personal relationships that could have appeared to influence the work reported in this paper.

Data availability

Data will be made available on request.

Acknowledgements

The authors would like to thank the Swedish Research Council for Environment, Agricultural Sciences and Spatial Planning (Formas) (Reg. No. 2017-00720) and the Swedish Government (N2017/07856/SUBT) for funding this research. TMA-drivers are acknowledged for protecting us from traffic when working on the highway. The Swedish Transport Administration, especially Tobias Ulegård, is acknowledged for support regarding Testsite E18 field work.

Appendix A. Supplementary material

Supplementary data to this article can be found online at https://doi.org/10.1016/j.envint.2022.107618.

References

Aguilera, A., Bautista-Hernández, D., Bautista, F., Goguitchaichvili, A., Cejudo, R., 2021. Is the Urban Form a Driver of Heavy Metal Pollution in Road Dust? Evidence from Mexico City. Atmosphere 12, 266. https://doi.org/10.3390/atmos12020266.

Amato, F., Schaap, M., Denier van der Gon, H.A.C., Pandolfi, M., Alastuey, A., Keuken, M., Querol, X., 2013. Short-term variability of mineral dust, metals and carbon emission from road dust resuspension. Atmos. Environ. 74, 134–140. https://doi.org/10.1016/j.atmosenv.2013.03.037.

Amato, F., Alastuey, A., de la Rosa, J., Gonzalez Castanedo, Y., Sánchez de la Campa, A. M., Pandolfi, M., Lozano, A., Contreras González, J., Querol, X., 2014. Trends of road dust emissions contributions on ambient air particulate levels at rural, urban and industrial sites in southern Spain. Atmos. Chem. Phys. 14, 3533–3544. https://doi.org/10.5194/acp-14-3533-2014.

Amato, F., Favez, O., Pandolfi, M., Alastuey, A., Querol, X., Moukhtar, S., Bruge, B., Verlhac, S., Orza, J.A.G., Bonnaire, N., Le Priol, T., Petit, J.F., Sciare, J., 2016. Traffic induced particle resuspension in Paris: Emission factors and source contributions. Atmos. Environ. 129, 114–124. https://doi.org/10.1016/j.atmosenv.2016.01.022.

Amato, F., Bedogni, M., Padoan, E., Querol, X., Ealo, M., Rivas, I., 2017. Characterization of Road Dust Emissions in Milan: Impact of Vehicle Fleet Speed. Aerosol Air Qual. Res. 17, 2438–2449. https://doi.org/10.4209/aaqr.2017.01.0017.

Arvidsson, A. K., Blomqvist, G., Stave, C., Wärme, M., Polukarova, M., Bäckström, A.,2021. Dynamisk prognosstyrd vinterväghållning – Fas 3 & 4. Restsaltmodeller och automatisk saltspridning. *Swedish National Road and Transport Research Institute, VTI.* Linköping, Sweden. VTI-result; 2021:4.

Baensch-Baltruschat, B., Kocher, B., Stock, F., Reifferscheid, G., 2020. Tyre and road wear particles (TRWP)–- A review of generation, properties, emissions, human health risk, ecotoxicity, and fate in the environment. Sci. Total Environ. 733, 137823 https://doi.org/10.1016/j.scitotenv.2020.137823.

Beddows, D.C.S., Harrison, R.M., 2021. PM10 and PM2.5 emission factors for non-exhaust particles from road vehicles: Dependence upon vehicle mass and implications for battery electric vehicles. Atmos. Environ. 244. https://doi.org/10.1016/j.atmosenv.2020.117886.

Boucher, J., Friot, D., 2017. Primary Microplastics in the Oceans: A Global Evaluation of Sources. International Union for Conservation of Nature. IUCN, Switzerland. https://doi.org/10.2305/IUCN.CH.2017.01.en.

Bykova, G.S., Umarova, A.B., Guo, P., Kleipikova, E.A., Zavgorodnyaya, J.A., 2021. Urban road dust properties and its effect on the model soil's wettability. IOP Conference Series: Earth and Environmental Science 862, 012040. https://doi.org/10.1088/1755-1315/862/1/012040.

Chae, E., Jung, U., Choi, S.S., 2021. Quantification of tire tread wear particles in microparticles produced on the road using oleamide as a novel marker. Environ. Pollut. 288 https://doi.org/10.1016/j.envpol.2021.117811.

Denby, B., Sudvor, I., Johansson, C., Pirjola, L., Ketzel, M., Norman, M., Kupiainen, K., Gustafsson, M., Blomqvist, G., Omstedt, G., 2013. A coupled road dust and surface moisture model to predict non-exhaust road traffic induced particle emissions (NORTRIP). Part 1: Road dust loading and suspension modelling. Atmos. Environ. 77, 283–300. https://doi.org/10.1016/j.atmosenv.2013.04.069.

Dröge, R., Tromp, P., 2019. Measurements of organic micropollutants, microplastics and associated substances from road transport. MICROPROOF Deliverable 6 (6). The Netherlands Organisation for Applied Sciences Research (TNO).

Fauser, P., Tjell, J.C., Mosbaek, H., Pilegaard, K., 1999. Quantification of tire-tread particles using extractable organic zinc as tracer. Rubber Chem. Technol. 72, 969–977. https://doi.org/10.5254/1.3538846.

Fomba, K.W., van Pinxteren, D., Müller, K., Spindler, G., Herrmann, H., 2018. Assessment of trace metal levels in size-resolved particulate matter in the area of Leipzig. Atmos. Environ. 176, 60–70. https://doi.org/10.1016/j.atmosenv.2017.12.024.

Fussell, J., Franklin, M., Green, D., Gustafsson, M., Harrison, R., Hicks, W., Kelly, F., Kishta, F., Miller, M., Mudway, I., Oroumiyeh, F., Selley, L., Wang, M., Zhu, Y., 2022. A Review of Road Traffic-Derived Non-Exhaust Particles: Emissions, Physicochemical Characteristics, Health Risks, and Mitigation Measures. Environmental Sciences and Technology 56, 11, 6813–6835. https://doi.org/10.1021/acs.est.2c01072.

Fuzzi, S., Baltensperger, U., Carslaw, K., Decesari, S., Denier van der Gon, H., Facchini, M.C., Fowler, D., Koren, I., Langford, B., Lohmann, U., Nemitz, E., Pandis, S., Riipinen, I., Rudich, Y., Schaap, M., Slowik, J.G., Spracklen, D.V., Vignati, E., Wild, M., Williams, M., Gilardoni, S., 2015. Particulate matter, air quality and climate: lessons learned and future needs. Atmos. Chem. Phys. 15, 8217–8299. https://doi.org/10.5194/acp-15-8217-2015.

Gelencsér, A., May, B., Simpson, D., Sánchez-Ochoa, A., Kasper-Giebl, A., Puxbaum, H., Caseiro, A., Pio, C., Legrand, M., 2007. Source apportionment of PM2.5 organic aerosol over Europe: Primary/secondary, natural/anthropogenic, and fossil/biogenic origin. Journal of Geophysical Research: Atmospheres 112. https://doi.org/10.1029/2006JD008094.

Goßmann, I., Halbach, M., Scholz-Böttcher, B.M., 2021. Car and truck tire wear particles in complex environmental samples – A quantitative comparison with "traditional" microplastic polymer mass loads. Sci. Total Environ. 773, 145667 https://doi.org/10.1016/j.scitotenv.2021.145667.

Gustafsson, M., Blomqvist, G., Järlskog, I., Lundberg, J., Janhäll, S., Elmgren, M., Johansson, C., Norman, M., Silvergren, S., 2019. Road dust load dynamics and influencing factors for six winter seasons in Stockholm, Sweden. Atmospheric Environment: X; 210. 1016/j.aeaoa.2019.100014.

Ha, S.Y., Kim, G.B., Yim, U.H., Shim, W.J., Hong, S.H., Han, G.M., 2012. Particle-Size Distribution of Polycyclic Aromatic Hydrocarbons in Urban Road Dust of Masan, Korea. Archivesof Environmental Contamination and Toxicology 63, 189–198. https://doi.org/10.1007/s00244-012-9765-4.

Halle, L.L., Palmqvist, A., Kampmann, K., Jensen, A., Hansen, T., Khan, F.R., 2021. Tire wear particle and leachate exposures from a pristine and road-worn tire to Hyalella azteca: Comparison of chemical content and biological effects. Aquat. Toxicol. 232, 105769 https://doi.org/10.1016/j.aquatox.2021.105769.

Hann, S., Sherrington, C., Jamieson, O., Hickman, M., Kershaw, P., Bapasola, A., Cole, G., 2018. Investigating options for reducing releases in the aquatic environment of microplastics emitted by (but not intentionally added in) products. *ICF and Eunomia Research & Consulting Ltd.* Report. [www] http://ec.europa.eu/environment/marine/good-environmental-status/descriptor-10/pdf/microplastics_final_report_v5_full.pdf. (available: 2022-09-02).

Hartmann, N.B., Hüffer, T., Thompson, R.C., Hassellöv, M., Verschoor, A., Daugaard, A. E., Rist, S., Karlsson, T., Brennholt, N., Cole, M., Herrling, M.P., Hess, M.C., Ivleva, N. P., Lusher, A.L., Wagner, M., 2019. Are We Speaking the Same Language? Recommendations for a Definition and Categorization Framework for Plastic Debris. Environ. Sci. Technol. 53, 1039–1047. https://doi.org/10.1021/acs.est.8b05297.

Järlskog, I., Strömvall, A. M., Magnusson, K., Gustafsson, M., Polukarova, M., Galfi, H., Aronsson, M., Andersson-Sköld, Y., 2020. Occurrence of tire and bitumen wear microplastics on urban streets and in sweepsand and washwater. Science of the total Environment; 72910. 1016/j.scitotenv.2020.138950.

Järlskog, I., Strömvall, A.-M., Magnusson, K., Galfi, H., Björklund, K., Polukarova, M., Garção, R., Markiewicz, A., Aronsson, M., Gustafsson, M., Norin, M., Blom, L., Andersson-Sköld, Y., 2021. Traffic-related microplastic particles, metals, and organic pollutants in an urban area under reconstruction. Sci. Total Environ. 774, 145503 https://doi.org/10.1016/j.scitotenv.2021.145503.

Järlskog, I., Jaramillo-Vogel, D., Rausch, J., Perseguers, S., Gustafsson, M., Strömvall, A.-M., Andersson-Sköld, Y., 2022. Differentiating and quantifying carbonaceous (tire, bitumen, and road marking wear) and non-carbonaceous (metals, minerals, and glass beads) non-exhaust particles in road dust samples from a traffic environment. Water Air Soil Pollut. 233, 375. https://doi.org/10.1007/s11270-022-05847-8.

Jeong, H., Choi, J.Y., Lim, J., Ra, K., 2020. Pollution Caused by Potentially Toxic Elements Present in Road Dust from Industrial Areas in Korea. Atmosphere. 2020; 11 (12):1366. 10.3390/atmos11121366.

Jonsson, P., Blomqvist, G., Gustafsson, M., 2008. Wet dust sampler : technological innovation for sampling particles and salt on road surface. Transportation Research Board 102–111. http://vti.diva-portal.org/smash/get/diva2:674043/FULLTEXT01.pdf.

Klein, M., Fischer, K., 2019. Microplastic abundance in atmospheric deposition within the Metropolitan area of Hamburg, Germany. Sci. Total Environ. 685, 96–103. https://doi.org/10.1016/j.scitotenv.2019.05.405.

Klöckner, P., Reemtsma, T., Eisentraut, P., Braun, U., Ruhl, A.S., Wagner, S., 2019. Tire and road wear particles in road environment – Quantification and assessment of particle dynamics by Zn determination after density separation. Chemosphere. https://doi.org/10.1016/j.chemosphere.2019.01.176.

Klöckner, P., Seiwert, B., Weyrauch, S., Escher, B.I., Reemtsma, T., Wagner, S., 2021. Comprehensive characterization of tire and road wear particles in highway tunnel road dust by use of size and density fractionation. Chemosphere 279, 130530. https://doi.org/10.1016/j.chemosphere.2021.130530.

Knight, L.J., Parker-Jurd, F.N.F., Al-Sid-Cheikh, M., Thompson, R.C., 2020. Tyre wear particles: an abundant yet widely unreported microplastic? Environ. Sci. Pollut. Res. 27, 18345–18354. https://doi.org/10.1007/s11356-020-08187-4.

Kole, J.P., Löhr, A.J., Van Belleghem, F.G.A.J., Ragas, A.M.J., 2017. Wear and tear of tyres: A stealthy source of microplastics in the environment. Int. J. Environ. Res. Public Health 14. https://doi.org/10.3390/ijerph14101265.

Kreider, M.L., Panko, J.M., McAtee, B.L., Sweet, L.I., Finley, B.L., 2010. Physical and chemical characterization of tire-related particles: Comparison of particles generated using different methodologies. Sci. Total Environ. 408, 652–659. https://doi.org/10.1016/j.scitotenv.2009.10.016.

Kumata, H., Yamada, J., Masuda, K., Takada, H., Sato, Y., Sakurai, T., Fujiwara, K., 2002. Benzothiazolamines as tire-derived molecular markers: Sorptive behavior in street runoff and application to source apportioning. Environ. Sci. Technol. 36, 702–708. https://doi.org/10.1021/es0155229.

Le Vern, M., Razakamanantsoa, A., Murzyn, F., Larrarte, F., Cerezo, V., 2021. Study on a test track of dust resuspension induced in a vehicle. International Transport and Air Pollution Conference 2021. Mar 2021, Graz, Austria. Hal-03272241v2.

Li, Y., Carlton, A.G., Shiraiwa, M., 2021. Diurnal and Seasonal Variations in the Phase State of Secondary Organic Aerosol Material over the Contiguous US Simulated in CMAQ. ACS Earth Space Chem. 5, 1971–1982. https://doi.org/10.1021/acsearthspacechem.1c00094.

Löder, M. G. J., Gerdts, G., 2015. Methodology Used for the Detection and Identification of Microplastics—A Critical Appraisal. In: Bergmann, M., Gutow, L., Klages, M. (eds) *Marine Anthropogenic Litter*. Springer, Cham. 10.1007/978-3-319-16510-3_8.

Lundberg, J., Blomqvist, G., Gustafsson, M., Janhäll, S., Järlskog, I., 2019. Wet Dust Sampler—a Sampling Method for Road Dust Quantification and Analyses. Water Air Soil Pollut. 230, 180. https://doi.org/10.1007/s11270-019-4226-6.

Lundberg, J., Gustafsson, M., Janhäll, S., Eriksson, O., Blomqvist, G., Erlingsson, S., 2020. Temporal Variation of Road Dust Load and Its Size Distribution—a Comparative Study of a Porous and a Dense Pavement. Water Air Soil Pollut. 231, 561. https://doi.org/10.1007/s11270-020-04923-1.

Mengistu, D., Heistad, A., Coutris, C., 2021. Tire wear particles concentrations in gully pot sediments. Sci. Total Environ. 769, 144785 https://doi.org/10.1016/j.scitotenv.2020.144785.

Mennekes, D., Nowack, B., 2022. Tire wear particle emissions: Measurement data where are you? Sci. Total Environ. 830, 154655 https://doi.org/10.1016/j.scitotenv.2022.154655.

Moghadam, S.G., Pazokifard, S., Mirabedini, S.M., 2021. Silane treatment of drop-on glass-beads and their performance in two-component traffic paints. Prog. Org. Coat. 156, 106235 https://doi.org/10.1016/j.porgcoat.2021.106235.

Mori, J., Fini, A., Galimberti, M., Ginepro, M., Burchi, G., Massa, D., Ferrini, F., 2018. Air pollution deposition on a roadside vegetation barrier in a Mediterranean environment: Combined effect of evergreen shrub species and planting density. Sci. Total Environ. 643, 725–737. https://doi.org/10.1016/j.scitotenv.2018.06.217.

Müller, A., Kocher, B., Altmann, K., Braun, U., 2022. Determination of tire wear markers in soil samples and their distribution in a roadside soil. Chemosphere 294, 133653. https://doi.org/10.1016/j.chemosphere.2022.133653.

NVDB., 2022. Vägtrafikflödeskartan. [www] https://vtf.trafikverket.se/SeTrafikinformation# . (available 2022-10-31).

Padoan, E., Amato, F., 2018. Chapter 2 - Vehicle Non-Exhaust Emissions: Impact on Air Quality. Non-Exhaust Emissions. Academic Press, 2018, pp. 21-65. 10.1016/B978-0-12-811770-5.00002-9.

Parker-Jurd, F.N.F., Napper, I.E., Abbott, G.D., Hann, S., Thompson, R.C., 2021. Quantifying the release of tyre wear particles to the marine environment via multiple pathways. Mar. Pollut. Bull. 172, 112897 https://doi.org/10.1016/j.marpolbul.2021.112897.

Piscitello, A., Bianco, C., Casasso, A., Sethi, R., 2021. Non-exhaust traffic emissions: Sources, characterization, and mitigation measures. Sci. Total Environ. 766, 144440 https://doi.org/10.1016/j.scitotenv.2020.144440.

Rasul, H., Earon, R., Olofsson, B., 2018. Detecting Seasonal Flow Pathways in Road Structures Using Tracer Tests and ERT. Water Air Soil Pollut. 229, 358. https://doi.org/10.1007/s11270-018-4008-6.

Rauert, C., Rødland, E.S., Okoffo, E.D., Reid, M.J., Meland, S., Thomas, K.V., 2021. Challenges with Quantifying Tire Road Wear Particles: Recognizing the Need for Further Refinement of the ISO Technical Specification. Environ. Sci. Technol. Lett. 8, 231–236. https://doi.org/10.1021/acs.estlett.0c00949.

Rausch, J., Jaramillo-Vogel, D., Perseguers, S., Schnidrig, N., Grobéty, B., Yajan, P., 2022. Automated identification and quantification of tire wear particles (TWP) in airborne dust: SEM/EDX single particle analysis coupled to a machine learning classifier. Sci. Total Environ. 803, 149832 https://doi.org/10.1016/j.scitotenv.2021.149832.

Rødland, E.S., Samanipour, S., Rauert, C., Okoffo, E.D., Reid, M.J., Heier, L.S., Lind, O.C., Thomas, K.V., Meland, S., 2022a. A novel method for the quantification of tire and polymer-modified bitumen particles in environmental samples by pyrolysis gas chromatography mass spectroscopy. J. Hazard. Mater. 423, 127092 https://doi.org/10.1016/j.jhazmat.2021.127092.

Rødland, E.S., Lind, O.C., Reid, M., Heier, L.S., Skogsberg, E., Snilsberg, B., Gryteselv, D., Meland, S., 2022b. Characterization of tire and road wear microplastic particle contamination in a road tunnel: From surface to release. J. Hazard. Mater. 435 https://doi.org/10.1016/j.jhazmat.2022.129032.

Schauer, J.J., Fraser, M.P., Cass, G.R., Simoneit, B.R.T., 2002. Source Reconciliation of Atmospheric Gas-Phase and Particle-Phase Pollutants during a Severe Photochemical Smog Episode. Environ. Sci. Technol. 36, 3806–3814. https://doi.org/10.1021/es011458j.

Shen, Z., Liu, J., Aini, G., Gong, Y., 2016. A comparative study of the grain-size distribution of surface dust and stormwater runoff quality on typical urban roads and roofs in Beijing, China. Environ. Sci. Pollut. Res. 23, 2693–2704. https://doi.org/10.1007/s11356-015-5512-5.

Sieber, R., Kawecki, D., Nowack, B., 2020. Dynamic probabilistic material flow analysis of rubber release from tires into the environment. Environ. Pollut. 258, 113573 https://doi.org/10.1016/j.envpol.2019.113573.

SMHI., 2022a. Average temperature. [www] https://www.smhi.se/data/meteorologi/ladda-ner-meteorologiska-observationer#param=airTemperatureMeanMonth,stations=core,stationid=97370. (available: 2022-10-31).

SMHI., 2022b. Annual average precipitation. [www] https://www.smhi.se/data/meteorologi/ladda-ner-meteorologiska-observationer#param=precipitationMonthlySum,stations=core,stationid=97370. (available 2022-10-31).

SMHI., 2022c.Wind speed and wind direction. [www] https://www.smhi.se/data/meteorologi/ladda-ner-meteorologiska-observationer/#param=wind,stations=all,stationid=97370. (available 2022-10-31).

Sommer, F., Dietze, V., Baum, A., Sauer, J., Gilge, S., Maschowski, C., Gieré, R., 2018. Tire Abrasion as a Major Source of Microplastics in the Environment. Aerosol Air Qual. Res. 18, 2014–2028. https://doi.org/10.4209/aaqr.2018.03.0099.

Svensson, N., Gustafsson, M., Blomqvist, G., 2022. Air quality at Testsite E18 : analyses of influencing factors. *Swedish National Road and Research Transport Institute, VTI.* Linköping, Sweden. VTI-report 1104.

Thomas, D., Schütze, B., Heinze, W.M., Steinmetz, Z., 2020. Sample Preparation Techniques for the Analysis of Microplastics in Soil—A Review. Sustainability 12, 9074. https://doi.org/10.3390/su12219074.

Thorpe, A., Harrison, R.M., 2008. Sources and properties of non-exhaust particulate matter from road traffic: A review. Sci. Total Environ. 400, 270–282. https://doi.org/10.1016/j.scitotenv.2008.06.007.

Unice, K.M., Kreider, M.L., Panko, J.M., 2013. Comparison of Tire and Road Wear Particle Concentrations in Sediment for Watersheds in France, Japan, and the United States by Quantitative Pyrolysis GC/MS Analysis. Environ. Sci. Technol. 47, 8138–8147. https://doi.org/10.1021/es400871j.

Verschoor, A., de Poorter, L., Dröge, R., Kuenen, J., de Valk, E., 2016. Emission of microplastics and potential mitigation measures- Abrasive cleaning agents, paints, and tyre wear. National Institute for Public Health and the Environment. Bilthoven, the Netherlands. RIVM Report 2016-0026. [www] https://www.rivm.nl/bibliotheek/rapporten/2016-0026.pdf. (available 2022-09-02).

Vogelsang, C., Kristiansen, T., Singdahl-Larsen, C., Buenaventura, N., Pakhomova, S., Eidsvoll, D. P., Staalstrøm, A., Beylich, B. A., 2020. Microplastic particles in and out of Bekkelaget wastewater treatment plant over one year. NIVA report 7541-2020: Norwegian Institute for Water Research, ISBN 978-82-577-7276-5. [www] https://hdl.handle.net/11250/2688601. (available 2022-11-02).

Wagner, S., Hüffer, T., Klöckner, P., Wehrhahn, M., Hofmann, T., Reemtsma, T., 2018. Tire wear particles in the aquatic environment - A review on generation, analysis, occurrence, fate and effects. Water Res. 139, 83–100. https://doi.org/10.1016/j.watres.2018.03.051.

Wang, C., O'Connor, D., Wang, L., Wu, W.-M., Luo, J., Hou, D., 2022. Microplastics in urban runoff: Global occurrence and fate. Water Res. 225, 119129 https://doi.org/10.1016/j.watres.2022.119129.

Wei, H., Muthanna, T.M., Lundy, L., Wiklander, M., 2022. An evaluation of temporal changes in physicochemical properties of gully pot sediments. Environ. Sci. Pollut. Res 29, 65452–65465. https://doi.org/10.1007/s11356-022-20341-8.

Wright, S.L., Ulke, J., Font, A., Chan, K.L.A., Kelly, F.J., 2020. Atmospheric microplastic deposition in an urban environment and an evaluation of transport. Environ. Int. 136 https://doi.org/10.1016/j.envint.2019.105411.

Xia, W., Rao, Q., Deng, X., Chen, J., Xie, P., 2020. Rainfall is a significant environmental factor of microplastic pollution in inland waters. Sci. Total Environ. 732, 139065 https://doi.org/10.1016/j.scitotenv.2020.139065.

Youn, J.S., Kim, Y.M., Siddiqui, M., Watanabe, A., Han, S., Jeong, S., Jung, Y.-W., Jeon, K.I., 2021. Quantification of tire wear particles in road dust from industrial and residential areas in Seoul, Korea. Sci. Total Environ. 784, 147177 https://doi.org/10.1016/j.scitotenv.2021.147177.

Yttri, K.E., Simpson, D., Bergström, R., Kiss, G., Szidat, S., Ceburnis, D., Eckhardt, S., Hueglin, C., Nøjgaard, J.K., Perrino, C., Pisso, I., Prevot, A.S.H., Putaud, J.P., Spindler, G., Vana, M., Zhang, Y.L., Aas, W., 2019. The EMEP Intensive Measurement Period campaign, 2008–2009: characterizing carbonaceous aerosol at nine rural sites in Europe. Atmos. Chem. Phys. 19, 4211–4233. https://doi.org/10.5194/acp-19-4211-2019.